NONCONTACT TENSION MEASUREMENT IN WEBS BY ACOUSTICAL POINT-SOURCE EXCITATION

By

MARLA ENFIELD BRADLEY

Bachelor of Science in Mechanical Engineering

Oklahoma State University

Stillwater, Oklahoma

1988

Submitted to the Faculty of the
Graduate College of the
Oklahoma State University
in partial fulfillment of
the requirements for
the Degree of
MASTER OF SCIENCE
December, 1989

NONCONTACT TENSION MEASUREMENT
IN WEBS BY ACOUSTICAL POINT-
SOURCE EXCITATION

Thesis Approved:

B. J. Lowery
Thesis Adviser

Gary E. Young

J. F. Leathrum

Norman N. Durham
Dean of the Graduate College

ACKNOWLEDGMENTS

I wish to extend my sincere thanks and appreciation to my adviser, Dr. Richard L. Lowery, for his encouragement and good advice throughout the course of this study. His understanding of acoustic phenomena has made this project very enlightening and interesting.

I also wish to thank Dr. J. Keith Good and Dr. Gary E. Young for serving as members of my graduate committee. Their suggestions for improving my thesis were invaluable.

Many thanks are extended to my husband, Bob, for his patience, understanding, and moral support. I also wish to thank my parents and parents-in-law for their moral support and encouragement.

TABLE OF CONTENTS

LIST OF TABLES

Table Page

LIST OF FIGURES

LIST OF SYMBOLS

c - Wave velocity in air

c_w - Wave velocity of a web in vacuum

c_φ - Wave velocity of an air-loaded web

k - Wave number for air

k_w - Wave number for a web in vacuum

K - Wave number for an air-loaded web

T - Tension per unit width of web

v_{ph} - Phase velocity

v_w - Web velocity

ω - Excitation frequency

ρ - Density of air

ρ_A - Mass of an air layer on a web

ρ_w - Areal density of the web

CHAPTER I

INTRODUCTION

The focus of this study has been on measurement of web tension. A web is considered to be a material manufactured and processed in a continuous, flexible strip form, such as paper, plastics, and textiles. Newspapers, paper and plastic bags, boxes, films, metal foil, floor coverings, and many more widely used products are manufactured with web handling processes.

Web tension varies in both time and space, thus reaching different momentary values in different portions of the web at any given time. All the rollers and elements in contact with the web cause tension disturbances, which can occur as continuous tension variations or tension peaks. Accurate web tension measurement is critical because tension variations and peaks lead to such problems as web breaks, web flutter, and wrinkles, which cause product and production time waste.

Most web breaks are caused by faults in web formation. When such a weak point occurs, web tension is not transferred at that point. The web breaks whenever the local stress, caused by an area of high tension, exceeds the tensile strength of the web at the weak point. Web breaks

can be both costly and dangerous on a high-speed production line.

Web flutter is a form of instability in the web which occurs when the web tension variations are in resonance with the web. The resonant frequency depends on the web geometry. Wrinkles can be due to a low-tension area in a cross-direction location of the web. Both wrinkles and flutter can be minimized by increasing the tension level, which improves the web stability. The cross-direction tension profile is valuable in identifying problem areas so that corrective action can be taken.

This study is based on the principle that the velocity of normal wave propagation in a web is related to the square root of the web tension. Different pulsers were used to propagate a wave down different types of webs. The wave was monitored at two different points in the web. From the distance between the two points and the time between the two signals, wave propagation velocity was calculated. In all cases, wave velocity increased with increasing tension. Use of a traversing mechanism across the web yielded the cross-direction tension profile. Both static and dynamic cases were considered.

CHAPTER II

LITERATURE REVIEW

Tension-Measuring Devices

The tension meters that have been developed in industry can be broadly classified into two major groups: those that contact the web (contacting) and those that do not touch the web (noncontacting). Descriptions of some industrial contacting tension sensors follow.

The Swedish Forest Products Laboratory (STFI) developed a contacting web tension sensor for cross-profile measurements on paper machines in 1978 (1). The measurement head is attached to the sheet by the use of vacuum apertures in a circular supporting ring. The web is excited to resonant frequency by a heated, temperature-controlled loudspeaker. A feedback control system keeps the web excited to resonance by measuring the phase difference between the input and output signal. The web tension is assumed to be proportional to the resonant frequency squared times the mass per unit area of the web. The measurement head scans the web, thus providing the tension profile.

In the mid-1980s, the Norwegian Pulp and Paper Research Institute (PFI) developed a contacting, portable, cross-direction web tension meter which consists of two parts: a

lightweight measuring head with a sensor in its center and a recording unit with digital display and a miniature pen recorder (2). A rechargeable battery pack supplies power to the instrument. The sensor in the measuring head is a curved steel spring blade that gently pushes into the web, causing a 1- or 2-mm indentation in the web. This indentation, which is measured by an inductive transducer, is dependent on the web tension. An LED signal informs the user if pressure against the web is insufficient. A calibration curve is necessary in order to convert the voltage signal, which is obtained from the spring blade's deflection, to the web tension.

Tidningspappersbrukens Forskningslaboratorium (TFL), a Swedish company, developed a contacting web tension meter utilizing a loudspeaker (3). The amplitude of the web from the loudspeaker acoustic waves at the measuring head is determined. This amplitude is a function of web tension. Frequency of tension variations can be obtained from a frequency analysis, which helps to determine the reasons for web tension disturbances.

Recent industry developments in noncontacting sensors will now be described.

A noncontacting web tension meter was developed in the USSR in the mid-1970s (1). Compressed air from an annular nozzle impinges on the paper web at an equal distance from two web-guiding rolls. A central pneumatic chamber experiences pressure oscillations from the transversal web

vibrations; these oscillations are picked up by a condenser microphone. The output signal is connected to a dynamic loudspeaker on the other web side, opposite the nozzle. This feedback keeps the loudspeaker at resonant frequency, which correlates with web tension. Cross-direction averaging was attained by modifying this system to use a multinozzle generator to oscillate the total width of the web and a proximity detector underneath the web (1).

In the mid-1980s, STFI developed a noncontacting sensor (4) based on the same principle as its above-described contacting sensor. The web is vibrated by a loudspeaker, and the phase difference between the input and output signal is used as feedback to keep the web in resonance. The resonant frequency corresponds to web tension by the equation:

$$f^2 = k * (Nx/w)$$

where f is the frequency, Nx is the web tension in the machine direction, w is the basis weight, and k is a constant. STFI claims a 5 percent relative error, where the maximum bending stiffness is 1 mNm (corresponding to basis weight of 100 g/m^2) and maximum web speed is 10 m/s (for basis weight less than 100 g/m^2).

Altim Control of Finland developed the Altim Tensometer, which is a contactless local tension-measuring device (3, 5), in the mid-1980s. A loudspeaker generates a

spatially confined sound burst, repeated once a second to avoid standing waves, which generates a wave front to the membrane. Two microphones on each side of the source monitor the wave propagation; they are placed at different distances from the source. The resulting time delay between the two signals is derived using cross-correlation for both signals. Since each side of the source has two microphones, web speed cancels out of the average wave velocity, because the web speed would be added to the upstream side of the source and subtracted from the downstream side of the source. This average wave velocity is used in empirical lookup tables based on basis weight to determine the local tension in the web.

The measuring head is on its own stand, and the equipment needs no calibration. Web tension is read directly in digital form in N/m or in analog form. Sampling rate is 15 milliseconds.

TENSCAN, which was developed in Finland in 1987, is a scanning tension profile measuring system which utilizes a loudspeaker to induce a wave onto a moving web (6). The system consists of a measuring head with a one-sided scanner frame and an operator station. The operator station contains a color monitor, dedicated keyboard, computer, power supplies, and a plotter. The measuring head consists of a laser, loudspeaker, and three optical sensors--two on one side of the sound burst and one on the other side. It

may be mounted on the scanner frame or used as a stand-alone unit.

The measuring head produces a sound burst at preset intervals as it scans the web. The sound wave induces a membrane wave which travels in the direction of the tension. The three optical sensors, or position-sensing arrays, convert movement of the laser's spot into three different electronic waveforms. The signals are then passed to the operator station, and the computer uses a cross-correlation function to determine time delay between the three waveforms. The farthest signal from one side of the sound burst and the signal on the other side of the sound burst are used to calculate web speed. The time difference between the two signals on the one side of the sound burst is then calculated, and the effects of web speed are subtracted out.

The distance between the measuring head and the web is measured by the lasers so that it can be considered in the tension calculation. Effects of web flutter and elasticity are eliminated by using the proper sound burst frequency. A correlation has been determined between tension and basis weight for all paper grades.

All of the above devices can easily measure cross-web tension profiles. Therefore, all of the devices are an improvement over the use of force transducers to measure the force created by a web passing over a roller, which has been the usual way to measure web tension in industry (7). The

force transducers show the average tension across the web. A rough cross-direction profile is obtained by dividing the web into several areas, which are measured separately.

Effects of Air Loading on Membrane Wave Velocity

In many elementary vibrations and acoustics textbooks, the equation relating tension and normal wave propagation velocity in a vacuum is found:

$$c_w = (T/\rho_w)^{1/2}$$

where c_w is the wave velocity, T is the tension, and ρ_w is the basis weight of the web. However, when the web is exposed to the atmosphere, air loading effects on the web must be taken into account to calculate the web wave velocity. The theory applies for a plane wave which exists across the entire width of the web. Jaihak Lee (8) adapted some equations which account for this air loading on webs from two sources (Morse et. al., Theoretical Acoustics, 1968, and Sabersky et. al., Fluid Flow, 1971). The equations involved the wave number for the air, k, and the wave number for the web in the air, K. He considered two cases; the first one was for $k < K$. This case implies no attenuation of the wave as it travels down the web. The equations are:

$$K = k_w \left[1 + \frac{2 * \rho}{\rho_w * (K^2 - k^2)^{1/2}} \right]^{1/2}$$

or

$$K^6 - (k^2 + 2k_w^2)K^4 + k_w^2(k_w^2 + 2k^2)K^2 - k_w^4[k^2 + (4 * \rho^2/\rho_w^2)] = 0$$

where K is the wave number for the web in the air, k_w is the wave number for the web in vacuo, k is the wave number for the air, ρ is the density of the air, and ρ_w is the areal density of the web. Lee used a value of ρ equal to 1.21 kg/m^3 (0.0755 lbm/ft^3). The wave number for the air, k, was calculated by:

$$k = 2 * \pi * f/c$$

where f is the frequency in hertz and c, the wave speed in air, was taken to be 343 m/s (1125 ft/s).

The wave velocity in the x direction can finally be calculated from the following equation:

$$c_\varphi = kc/K = \omega/K$$

where ω is the excitation frequency.

Case 2, when k > K, implies that energy radiates away from the medium and that the wave attenuates in the x direction. The wave number K now is an imaginary number. This case is impossible because it implies that speed of sound in the web is greater than that in the air. The

equations are:

$$K^2 = k_w^2 \left[1 + i \frac{2 * \rho}{\rho_w * (k^2 - K^2)^{1/2}} \right]$$

or

$$K = k_w \left[1 + i \frac{2 * \rho}{\rho_w * (k^2 - K^2)^{1/2}} \right]^{1/2}$$

If the imaginary term has a magnitude much less than 1, the above equation becomes:

$$K = k_w \left[1 + i \frac{\rho}{\rho_w * (k^2 - K^2)^{1/2}} \right]$$

The velocity in the x direction now is:

$$c_\varphi = kc/Re(K) = kc/k_w = c_w$$

Lee found that, for typical webs and tensions, the wave speed approaches $(T/\rho)^{1/2}$ as frequency approaches 10 kilohertz. Therefore, if a high-frequency signal could be generated, the wave equation for the air-loaded web would not have to be utilized.

Previous Research

Glen Francis (9) investigated the variance of normal wave propagation velocity with respect to variations of tension in a static web. He used three different speakers for pulse transducers--a line array of 3.5-inch "wolfer"

speakers, a line piezo-type tweeter, and an 0.75-inch hard dome tweeter. A coherent gate (tone burst generator) was used with the speakers to generate pulse packets. An amplifier was placed between the oscillator and the pulse transducer, and the signal was picked up down the web by a microphone. The time delay between the signal being sent to the pulse transducer and the signal being received by the microphone was determined, and the wave velocity was calculated from the time difference. Francis' findings were that (1) as frequency increases, the effect of air mass decreases and (2) as tension increases, the effect of air mass increases. These findings follow from the fact that wavelength grows longer as air mass increases. Additional findings were:

1. The trace contained an initial high-frequency portion which was due to the sound moving through the air and reaching the sensor before the signal in the web.

2. As the distance from the pulser to the microphone increased, this high-frequency signal due to sound in the air dispersed much faster than the lower-frequency web signal because of its higher velocity.

3. The pulse attenuated with increasing microphone distance.

4. The higher the frequency was, the faster the signal attenuated.

5. Because of the signal attenuation, the larger the distance was between the pulse transducer and the receiving transducer, the more difficult it was to make accurate measurements.

Darin W. Nutter (10) developed an air pulse technique in which a pneumatic device was used to send a shock wave, or air pulse, onto the web. Two microphones, downstream from the air pulse, each picked up a signal; the time between the two signals was used to calculate the wave speed. The web tension was computed using the wave speed equation in vacuum:

$$T = \rho * c^2$$

where T is tension per unit width of the web, ρ is the basis weight (areal density) of the web, and c is the wave propagation velocity.

The results showed measured tensions correlating with actual tension within 5.7 percent in a polypropylene web. The pulse created by the pneumatic device was very short and crisp--one millisecond in duration and only one cycle, making it easy to distinguish from noise. The pulse did attenuate with distance, meaning that air loading effects on the web should be considered.

CHAPTER III

THEORY

Theoretically, a web is considered to be a membrane which vibrates with a small displacement and is thin and uniform with negligible stiffness. This membrane can be modeled as an assemblage of parallel strings. These strings contain waves whose crests are in parallel lines, perpendicular to their direction of propagation. These waves behave like waves on a flexible string; they travel with unchanged shape and equal speed. The two-dimensional wave equation is used to model the system, and the wave velocity for the web in-vacuo becomes:

$$c = (T/\rho)^{1/2}$$

However, the wave motion that the membrane has is not usually this simple. Under atmospheric conditions, the dispersive relationship when the membrane is coupled to air must be considered (11). This derivation can be done by adding the reactive force of air to the wave equation and employing continuity conditions on the surface. The energy carried by the coupled system is trapped within the membrane, and attenuation of the wave is assumed to arise

from viscous and thermal conductivity losses on the membrane surface.

Following the derivation procedure, the dispersion relation for membrane waves coupled to air becomes:

$$\omega^2 = \frac{c_m^2 * K^2}{1 + \frac{2 * \rho}{\sigma * (K^2 - k^2)^{1/2}}}$$

where ω is the frequency, $c_m = (T/\sigma)^{1/2}$ is the vacuum membrane wave velocity, K is the wave number for the membrane in air, ρ is the density of the air, σ is the areal density of the membrane, and k is the wave number for the air. When ρ goes to zero, the phase velocity v_{ph}, which equals ω/K, will really be c_m.

The dispersion can thus be explained as a mass loading effect so that the mass of air within the wave is added to the membrane mass. At low frequencies, the effective membrane mass is increased and the wave propagates more slowly.

The group velocity of the wave is obtained by taking the derivative of the equation for frequency, $d\omega/dK$. The group velocity is the component of the plane wave velocity along the waveguide axis, which is the speed at which the most significant portion of the pulse propagates. The expression for group velocity is:

$$v_{gr} = v_{ph} \left[1 + \frac{2 * \rho * \omega^2}{T * q^3} \right]$$

where q is $(K^2 - k^2)^{1/2}$. This equation means that the group velocity will always be somewhere between the phase velocity and velocity in vacuum.

All of the above theory applies to a so-called ribbon wave, which exists across the entire width of the web. The pneumatic wave generated in this study was a point-source shock wave. Most theory centers around a small-amplitude wave. The wave generated by the pneumatic pulser was probably too large to effectively utilize such theory, and it became shorter and wider as it propagated, therefore exhibiting nonlinearity.

Nonlinear acoustics theory studies the propagation of an acoustic wave of finite amplitude in a dissipative medium (12). The presence of viscosity and thermal conduction in media requires account of dissipation of energy in the propagation of the waves. In this case, the shape of the wave is distorted and becomes quasi-discontinuous. Upon further propagation, the wave front becomes "washed out," and its thickness increases in proportion to the distance. Eventually, the shape of the wave becomes almost sinusoidal.

Marttinen and Luukkala (5) gave another expression for phase velocity which is convenient because it includes tension:

$$v_{ph} - v_w = \left[\frac{T}{\rho_w + \left(\frac{2 * \rho}{(K^2 - k^2)^{1/2}} \right)} \right]^{1/2}$$

where v_w is the web velocity, T is the tension per unit width of the web, ρ_w is the areal density of the web, ρ is the density of air, K is the wave number for the web in the air, and k is the wave number for the air. If the term

$$\frac{2 * \rho}{(K^2 - k^2)^{1/2}}$$

is called a constant, ρ_A, then the phase velocity becomes

$$v_{ph} - v_w = \left[\frac{T}{\rho_w + \rho_A}\right]^{1/2}$$

The term ρ_A describes the air load on the web. It is the increase of the basis weight by adding the mass of a layer of air of thickness $1/(K^2 - k^2)^{1/2}$ on both sides of the web. This term increases with increasing tension and, therefore, longer wavelength.

CHAPTER IV

OBJECTIVES

The objective of this study was to progress toward the development of an accurate on-line tension-measuring device. The device was to be noncontacting so that webs that could not be touched without damage--e.g., magnetic coated films--could benefit from its use. A light, compact, hand-held device would have advantages over some of the devices used in industry.

Different means of pulsing the web were to be explored in order to obtain the optimum pulse. Two different designs of pneumatic pulsers were used, as well as an electric spark gap pulser. Microphone spacing from the source and microphone spacing from the web were to be optimized, as well as length and diameter of tubing from the pulser to the web.

The best signal processing method was also to be found in order to obtain the most accurate time interval measurement. Also, the best way to measure the time interval was to be found. The cursor on a digital oscilloscope and a counter-timer were to be compared against the standard method of cross-correlation to find the time interval.

Averaged tension profile measurements were to be compared against actual average tension. The tension equation could then be calibrated to be equal to the average tension. An propagating error analysis was to be done to determine possible error in the load cell model due to measurement of different angles of the web on the frame.

Wave velocities were to be compared to those calculated using the previously mentioned formulas (5, 8). A sensitivity analysis for wavelength was to be done in order to determine how big the deviation would be if a constant wavelength were used in these formulas.

Another objective was to determine ρ_A, as described in Chapter III, Theory, for this particular device to substitute into the equation:

$$T = (v_{ph} - v_w)^2 * (\rho_w + \rho_A)$$

where T is the tension per unit width of the web, v_{ph} is the phase velocity, v_w is the web velocity, ρ_w is the basis weight of the web, and ρ_A is the weight of the air layer on the web. The term ρ_A was to be determined by solving the above equation for ρ_A:

$$\rho_A = \frac{T_{avg}}{(v_{ph} - v_w)^2} - \rho_w$$

The average tension T_{avg} was to be used to solve for ρ_A.

CHAPTER V

EXPERIMENTAL APPARATUS

Web Test Frames

Two web test frames were used in the experiments. The first was a static web support consisting of a metal frame. The apparatus is shown in Figure 1:

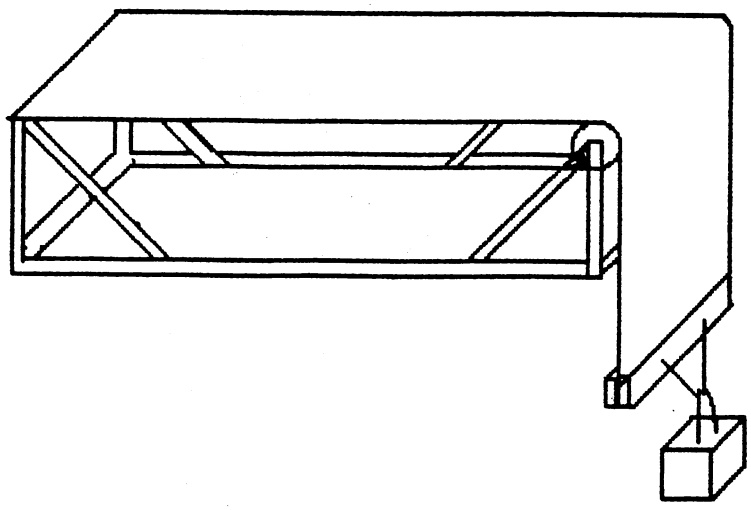

Figure 1. Static Web Frame

The frame is approximately two feet high, two feet wide, and six feet long. It was placed on a table so that weights on one end of the web would hang freely. As can be

seen from the figure, the web was attached to one end of the frame and ran across the length of the frame and over a roller. Two wooden brackets were clamped around the end of the web with several bolts. Weights were attached to the brackets using a hanger; the weights provided a known average tension in the web. However, the actual tension in the web was not necessarily uniform. The transducers were clamped under the web during the experiments.

The second system was a high-speed loop machine. This loop machine is shown in Figure 2 on the following page. The specifications on the machine are a speed of 12,000 feet per minute (fpm), tensions of 0.5 to 5 pounds per linear inch (pli), and web widths of 4 to 12 inches. It has 16 roll locations on each column and 24 column locations on the base. The rolls were rearranged so that the tension-measuring device could be placed under the lower loop of the web.

A traversing mechanism was built on which to mount the pulser tube and sensors. This mechanism is shown in Figure 3. The traverse, which has a 12-inch sidelay, was built for the purpose of obtaining a cross-direction tension profile. Once optimum distances were determined for microphone placement, a microphone and pulser tube holder with constantly spaced holes was built to be placed on only one of the microphone holders.

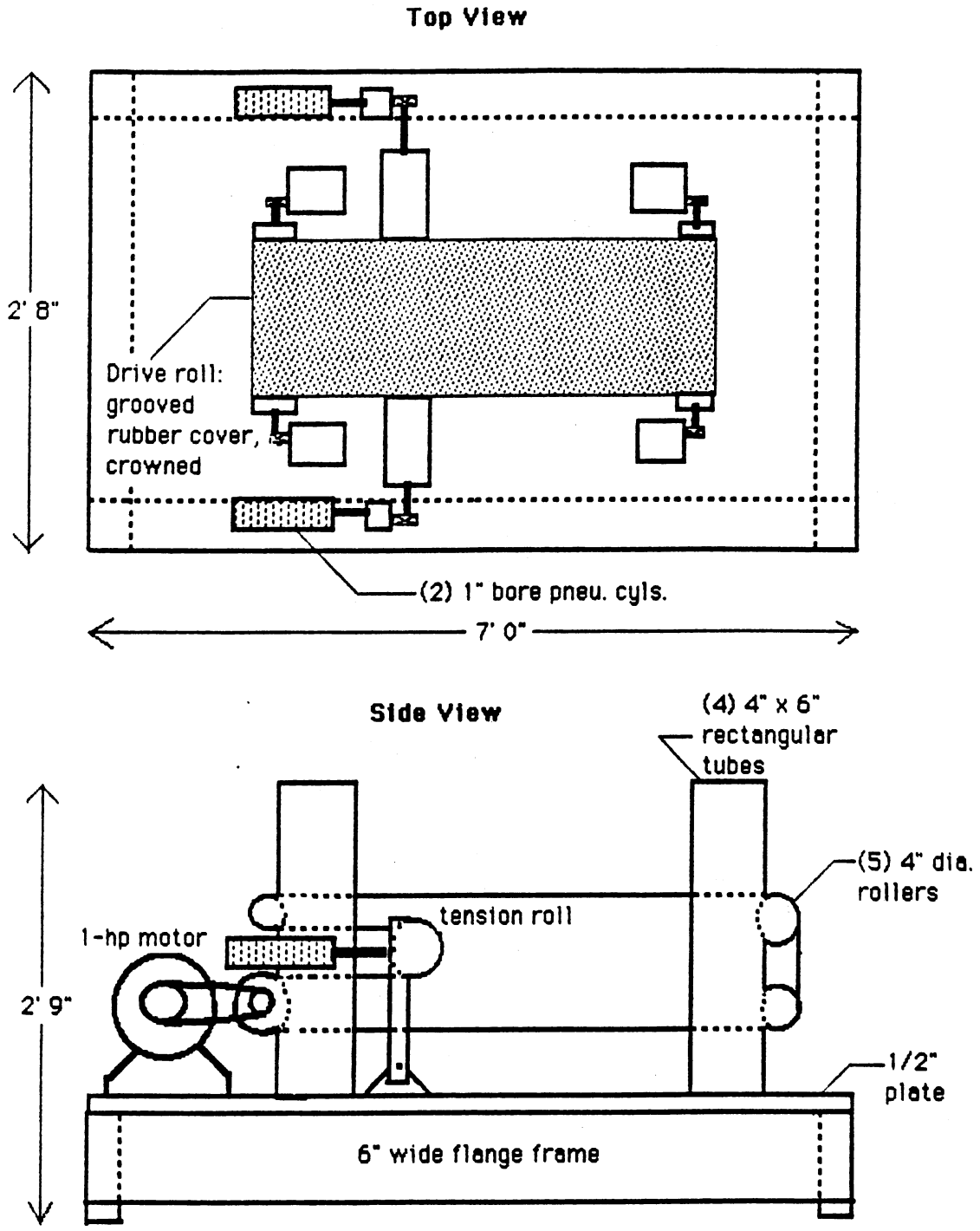

Figure 2. Endless Loop Machine

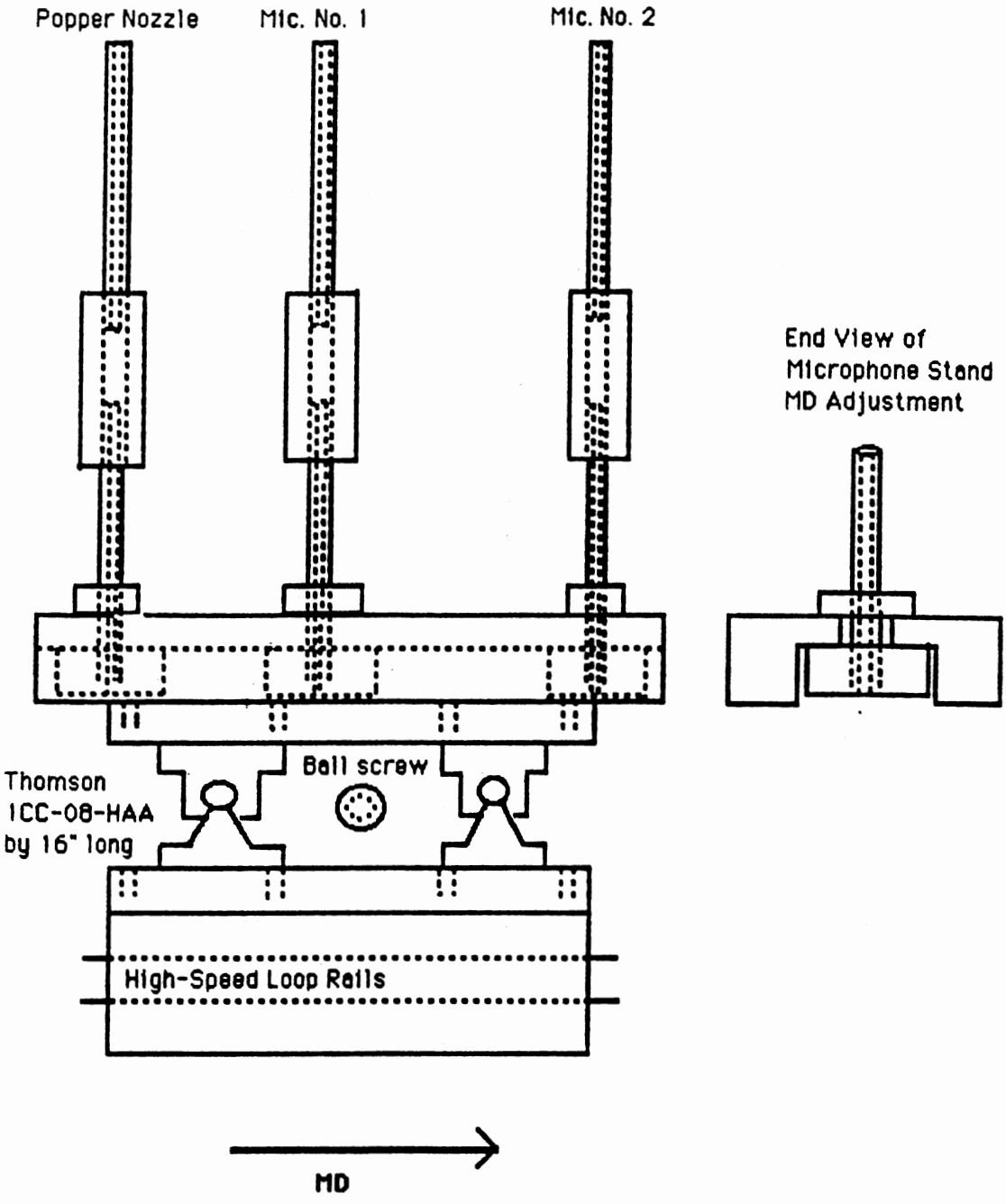

Figure 3. High-Speed Loop Traverse and Microphone Holders

Methods of Signal Generation

Several different methods of creating a wave in the web were explored. The first device is a pneumatic pulse generator which creates a shock wave; it is shown in Figure 4. This device consists of an aluminum disk with a hole in its edge rotating through a slot in an aluminum block. The aluminum block has a brass bushing inside to minimize resistance. The air source (120 psi) goes into the aluminum block, and when the hole in the disk rotates through the block, a pulse is created. The pulse is routed to the bottom of the web via 1/4-inch plastic tubing.

The disk is rotated by a Variac-controlled, 1/18-horsepower Bodine electric motor for ease of pulse rate control. The disk is 4 inches in diameter and 0.16 inch thick. The hole, which is drilled 0.2 inch from the edge of the disk, is 0.11 inch in diameter.

The second pulse-generating device is also a rotary pneumatic pulser, which is shown in Figure 5. A steel sawblade with a hole in its edge rotates through a pair of spring-loaded sliders, also with holes through their centers. The disk is driven by a 100-rpm, 1/4-horsepower Bodine gearmotor. The sliders and springs are pushed against the disk by brackets, which are bolted to the base. The tube from the air source (about 80 psi) comes into one slider, and tubing from the other slider goes to the bottom side of the web to create a pulse.

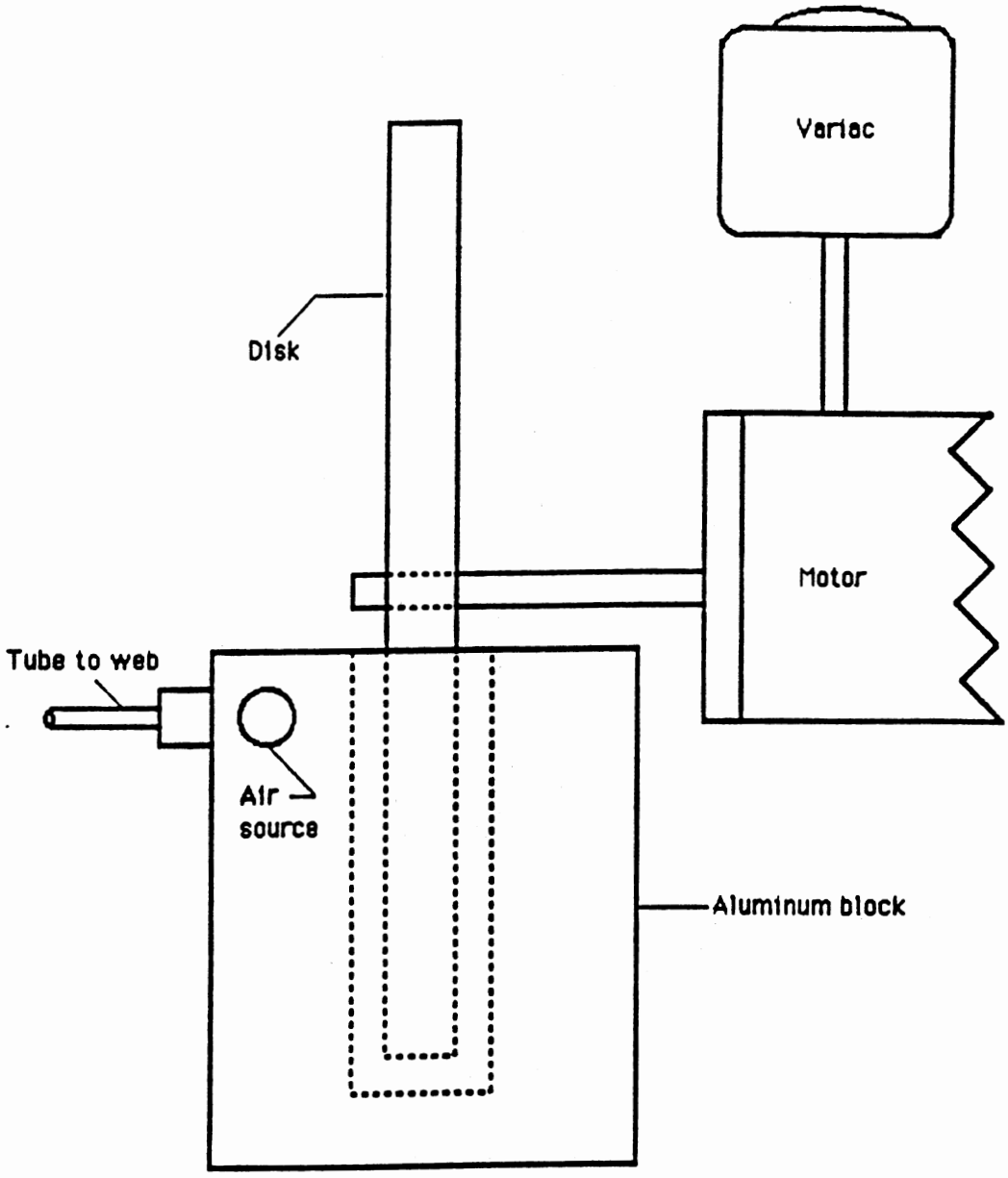

Figure 4. Original Pneumatic Air Pulser

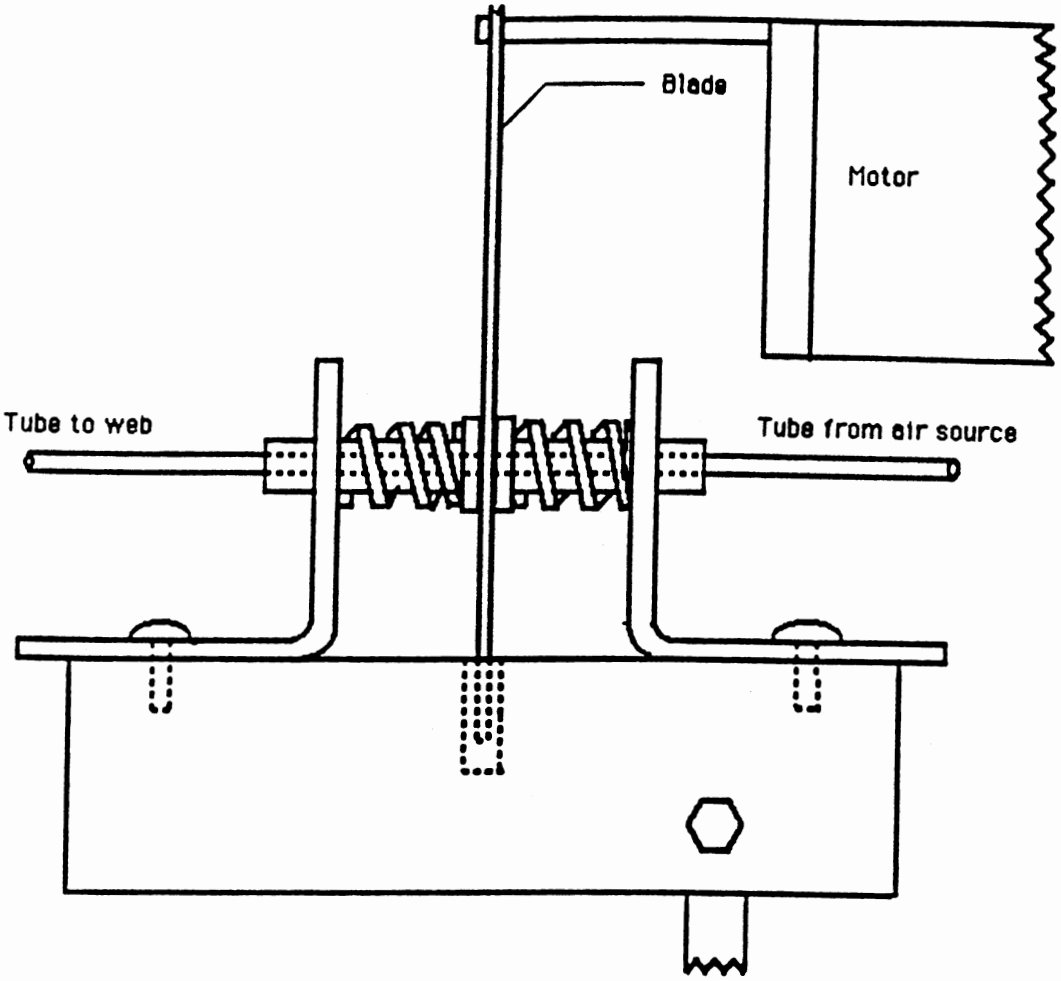

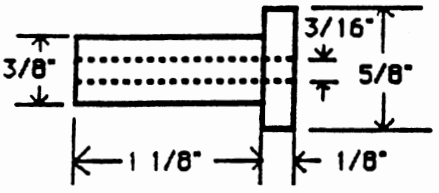

Figure 5. Pneumatic Pulser Design

The sliders are made of Delrin, which is good for minimizing wear and friction. The sliding portion is 5/8 inch in diameter and 1/8 inch thick. The sliders are 1 1/8 inches long and 3/8 inch wide, and the diameter of the hole drilled through them is 3/16 inch. The blade has a thickness of 1/16 inch and a radius of 4 1/2 inches. The hole in the blade is 3/16 inch in diameter and is drilled 5/8 inch from the edge of the blade. The plastic tubing has a 3/16-inch OD and a 3/32-inch ID.

An electric spark gap pulser was also tried as a pulse-producing method. Figure 6 shows the circuit associated with this pulser. The output of the circuit was routed to the web via a 5/8-inch-diameter tube.

Instrumentation for Data Collection

Two instruments were used to sample data. The first was the Analogics Data Precision DATA 6100 Digital Waveform Analyzer. This machine has a maximum sampling rate of 10 microseconds, or 100 kilohertz, per channel. With two channels enabled, the maximum sampling rate is 20 microseconds or 50 kilohertz. Four channels are available on the machine. The instrument is capable of taking the cross-correlation of two signals and the Fast Fourier Transform of a signal. The maximum and minimum of a signal can be found from buttons on the keyboard, and a cursor on the time scale is available to find where the maximum and minimum occur. A low-pass filter may be utilized for anti-

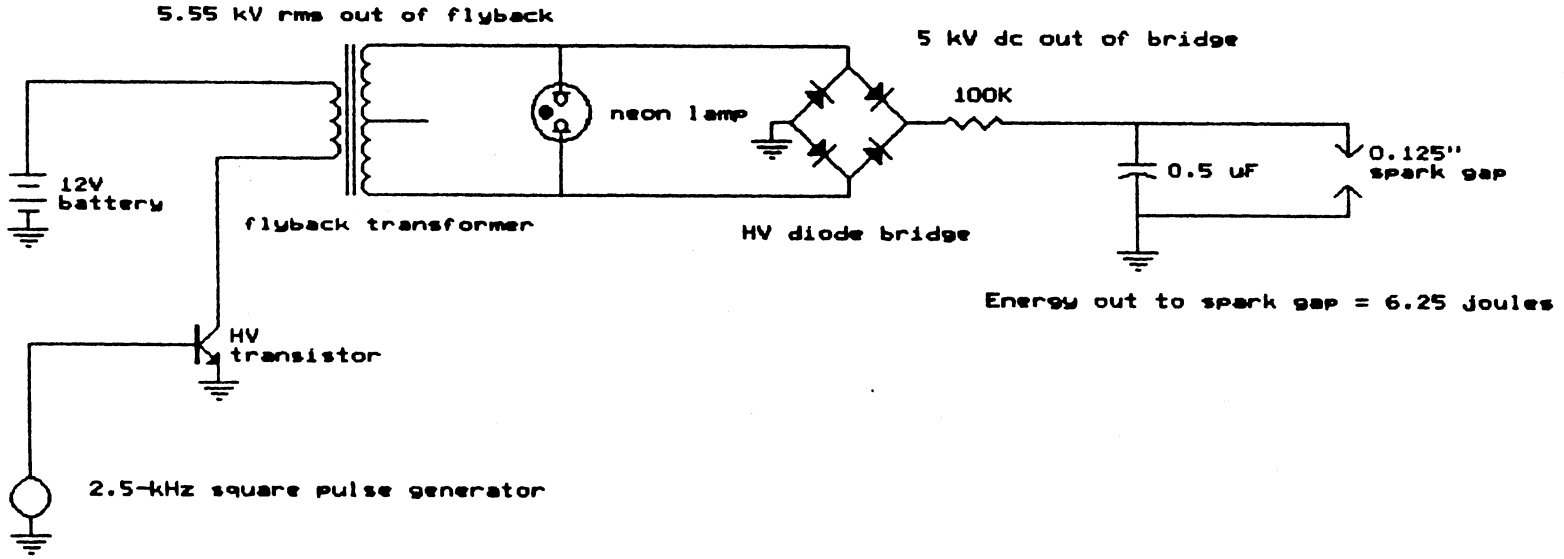

Figure 6. Spark Gap Pulser Circuit

aliasing purposes, and ac coupling eliminates any dc offset present. A disk drive can be connected to the DATA 6100 and data stored on disk. A plotter can also be connected to it for a hard copy.

The second instrument used was the Hewlett-Packard 54501A Digital Oscilloscope. This oscilloscope has a sampling rate of 10 megasamples per second. Like the DATA 6100, it also contains four channels. Storage capabilities are present in this instrument, and it contains cursors for measuring time distances and voltage distances. The machine prints delta t and delta V on the screen. It has a fine adjustment for measuring voltages. A printer is connected to it so that hard copies can be obtained.

Signal-Processing Methods

Three different signal-processing circuits were built to see which one gave the optimum signal, and thus the optimum time difference. The circuit descriptions and purposes follow.

The first circuit is a high-pass filter circuit, which is shown in Figure 7. The filter, which is actually a differentiator, has a summer following it for inversion and signal modification purposes. The circuit has a gain of 10 and a break frequency of about 160 hertz to eliminate low-cycle noise. The differentiator is meant to sharpen the signal by giving its slope. The summer adds the signal from the differentiator to 5 volts going through a potentiometer,

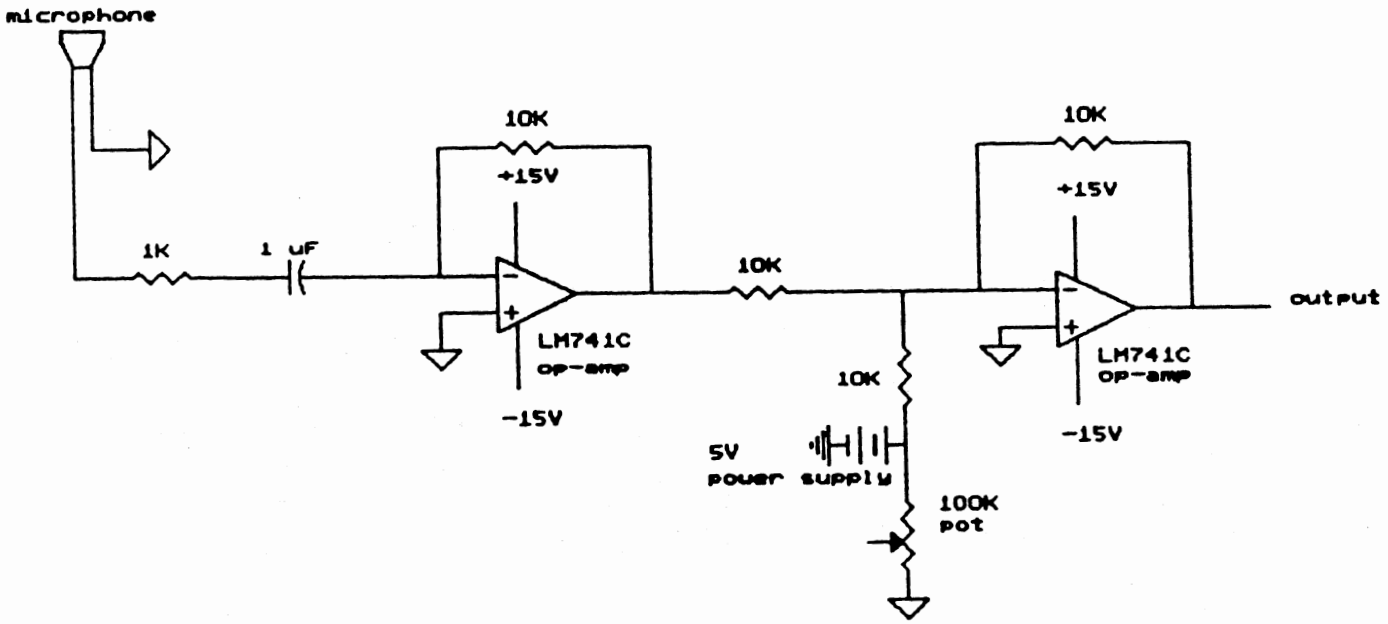

Figure 7. High-Pass Filter and Inverter

by which the signal can be modified. The summer also reinverts the signal, which is inverted by the differentiator.

The second circuit utilizes a Schmitt trigger. This circuit is shown in Figure 8. The basis of the circuit is the above-described high-pass filter circuit. Added to this circuit is a Schmitt trigger, which turns off at a voltage level of 1.6 volts and on at 0.8 volts. Thus it creates an inverted square wave by which the time difference between two signals can be measured. This circuit also has a gain of 10 and a break frequency of about 160 hertz.

Figure 9 shows the third circuit, which is called a Precision Diode Circuit. This circuit has a gain of 5. It eliminates any negative voltages by use of a diode. At the beginning of the experimental signals, a high-frequency negative pulse exists; this pulse is due to the noise from the sound in the air reaching the microphone before the web signal does. The positive-voltage web signal then follows. This circuit therefore eliminates the air spike in the signal and allows the signal in the web through.

Methods for Measuring Time Differences

Two ways to measure time differences were compared: (1) using the cursors on the Fourier analyzer and digital oscilloscope and (2) using a Hewlett-Packard 5314A counter-timer.

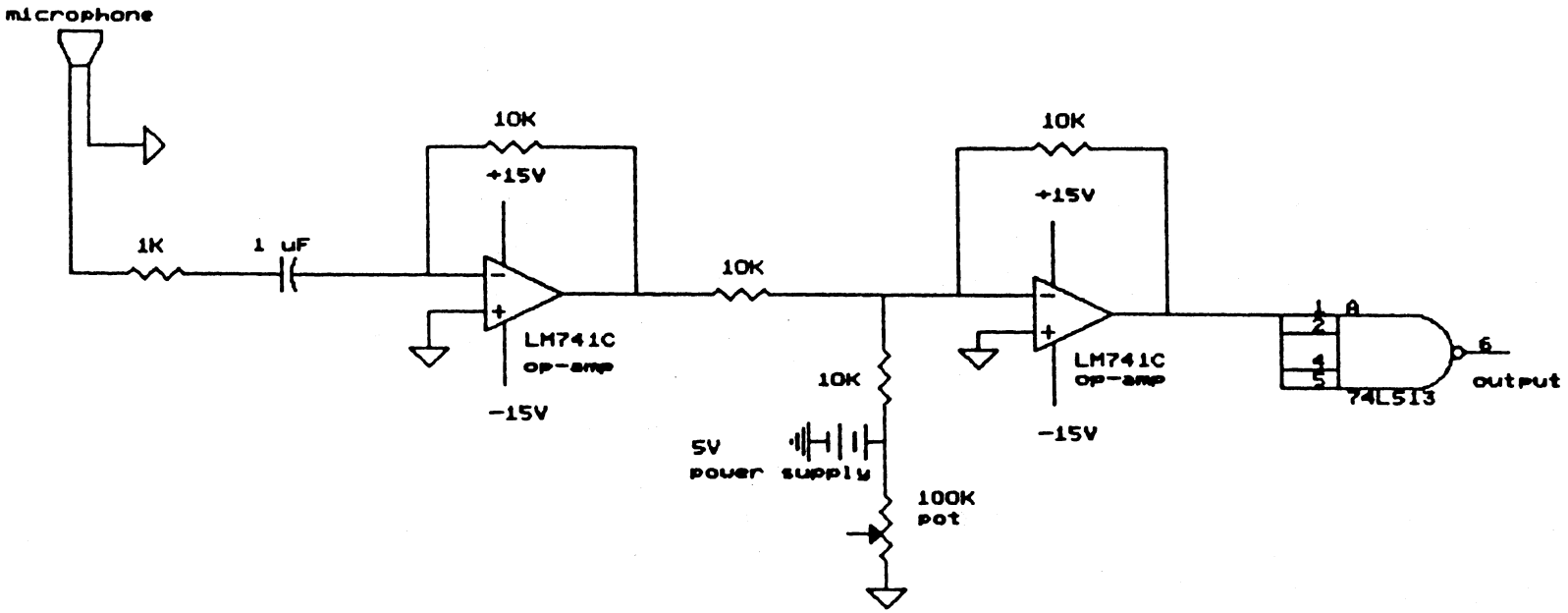

Figure 8. Schmitt Trigger Circuit

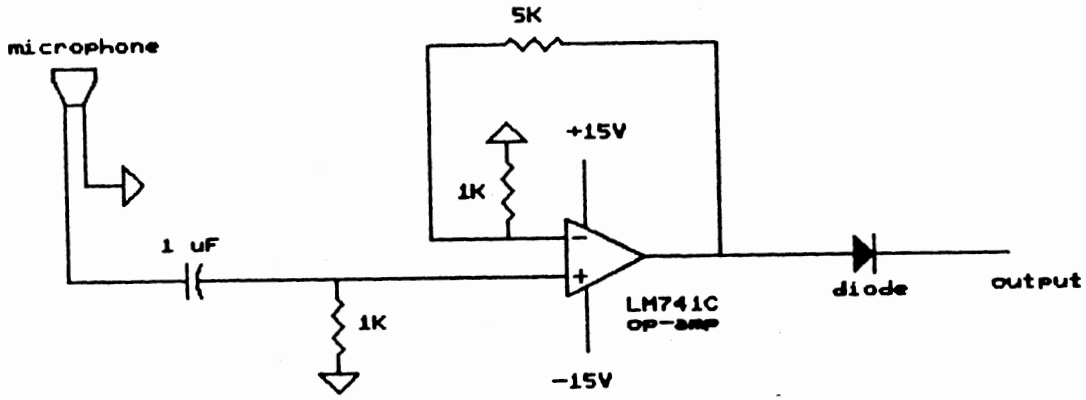

Figure 9. Precision Diode Circuit

As mentioned previously, the two instruments used for data collection contain cursors. One cursor can be set at the maximum of the first voltage signal, and the other cursor is set at the maximum of the second voltage signal. On the Fourier analyzer, the times associated with the maxima must be subtracted from one another to obtain the time difference between the two signals. On the digital oscilloscope, the screen automatically reads out a delta t.

The counter-timer can be set to trigger at levels as high as 300 millivolts for a positive or negative slope. It contains a button for time from A to B. The timer turns on at a certain voltage level of Signal A and turns off at a certain voltage level of Signal B. The time difference is displayed as a digital readout.

CHAPTER VI

RESULTS AND DISCUSSION

Microphone Calibration

The electret microphone elements were calibrated using a pistonphone calibrator. The pistonphone has an output of 124 decibels when it is connected to a 9-volt battery. The microphone is inserted into the pistonphone, and its output voltage is determined using the Fourier analyzer or digital oscilloscope. The zero-to-peak voltage is used to calculate the change in decibels from 124; i.e.,

$$dB = 20 \log_{10}(E)$$

$$\text{change in } dB = 20 \log_{10}(E_1/E_2)$$

where E is the voltage.

In the case of the two electret microphones, their output voltages measured 0.54 and 0.32 volts peak-to-peak. Using these numbers, it was determined that the microphones put out about 119 decibels in typical operation. Therefore, background factory noise will not affect the performance of the tension-measuring device, because typical factory noise is limited to 90 decibels by OSHA regulations.

Determination of Material Properties

The web materials used on the static web frame were 14 7/8-inch-wide paper and 15 7/16-inch-wide transparent polypropylene. Three-mil-thick paper and 1.4-mil-thick metallized web (coated with aluminum) were used on the high-speed loop machine. The width of these webs was 6 inches. The basis weights of all these materials were determined by cutting a large amount of each--about 20 square feet--and weighing each sample of material on a chemical scale for good accuracy. The weight in grams was converted to pounds mass and was then divided by the area of material measured. This calculation yielded the areal density, or basis weight.

The basis weight of the wide paper used on the static frame was estimated at 10.0×10^{-3} lbm/ft^2, and that of the wide polypropylene was 0.00617 lbm/ft^2. The 6-inch paper web used on the high-speed loop machine had a basis weight of 0.01557 lbm/ft^2, and the metallized web had a basis weight of 0.006801 lbm/ft^2.

Determination of Optimum Microphone Distances

Experiments were run to determine wave properties when microphones were placed at varying distances from the source. When the point source pulse hits the web, the pulse disperses; an analogy to this situation is when a stone hits a lake. Therefore, the closer the microphones are to the source, the better the received signal will be, because it

disperses rapidly. The peak of the signal became difficult to discern when placing it about 6 inches from the source. Thus the optimum setup was determined to be one microphone placed 2 inches downstream of the source and the second microphone placed 4 inches downstream of the source.

Effects of Tubing Rigidity and Length

The tubing which ran from the pulser to the web had an effect on the signal recorded by the microphones. Three different types of tubing were evaluated: (1) black rubber tubing, (2) plastic Tygon tubing, and (3) a plastic tube much harder than the Tygon tubing. The black rubber and plastic Tygon tubing were fairly soft. The microphone signal for the hard plastic tubing was sharper and narrower than the signals from the two softer tubes. The softer tubes may have damped out part of the signal.

A change in the signal was also noted with a change in length of the tubing. A long piece of tubing was inclined to give a less sharp, clear signal than a shorter tube. The wave tended to die out with the more distance it had to travel.

The tubing that was chosen for use was the hard plastic tubing. It was cut off to minimize the distance between the pulser and the web.

Wave Duration and Wave Height Tests

At the beginning of this research, it was determined

that the signals recorded by the microphones changed with changing tension. The signals became shorter in duration and had a higher peak voltage with increasing tension. This phenomenon is in contrast with acoustic theory, which states that acoustic waves should decrease in height with increasing tension. One possible explanation could be that the pulser tube interacts with the web in some way, because they are in very close proximity.

Some examples of this phenomenon will now be discussed. On the static frame (shown in Figure 1), paper and transparent polypropylene were the materials utilized. The original pneumatic pulser, which was discussed in Chapter 5 and shown in Figure 4, was the mechanism used to pulse the web. The pulser tube and microphones were placed below the web. The supply pressure into the pulser was approximately 120 psi.

Figure 10 on the next page, which is a series of recordings from the Fourier analyzer, shows the pulse increasing in height and decreasing in width with increasing tension for the 14 7/8-inch paper web. With a tension range of 0.672 to 1.68 pli, the pulse height varies from about -0.12 to -0.2 volts. Figure 11 shows the same phenomenon occurring for the 15 7/16-inch polypropylene web. With a tension range of 0.324 to 1.62 pli, the pulse height varies from about -0.2 to -0.4 volts. The microphone used for these recordings was 4 inches from the pulse source.

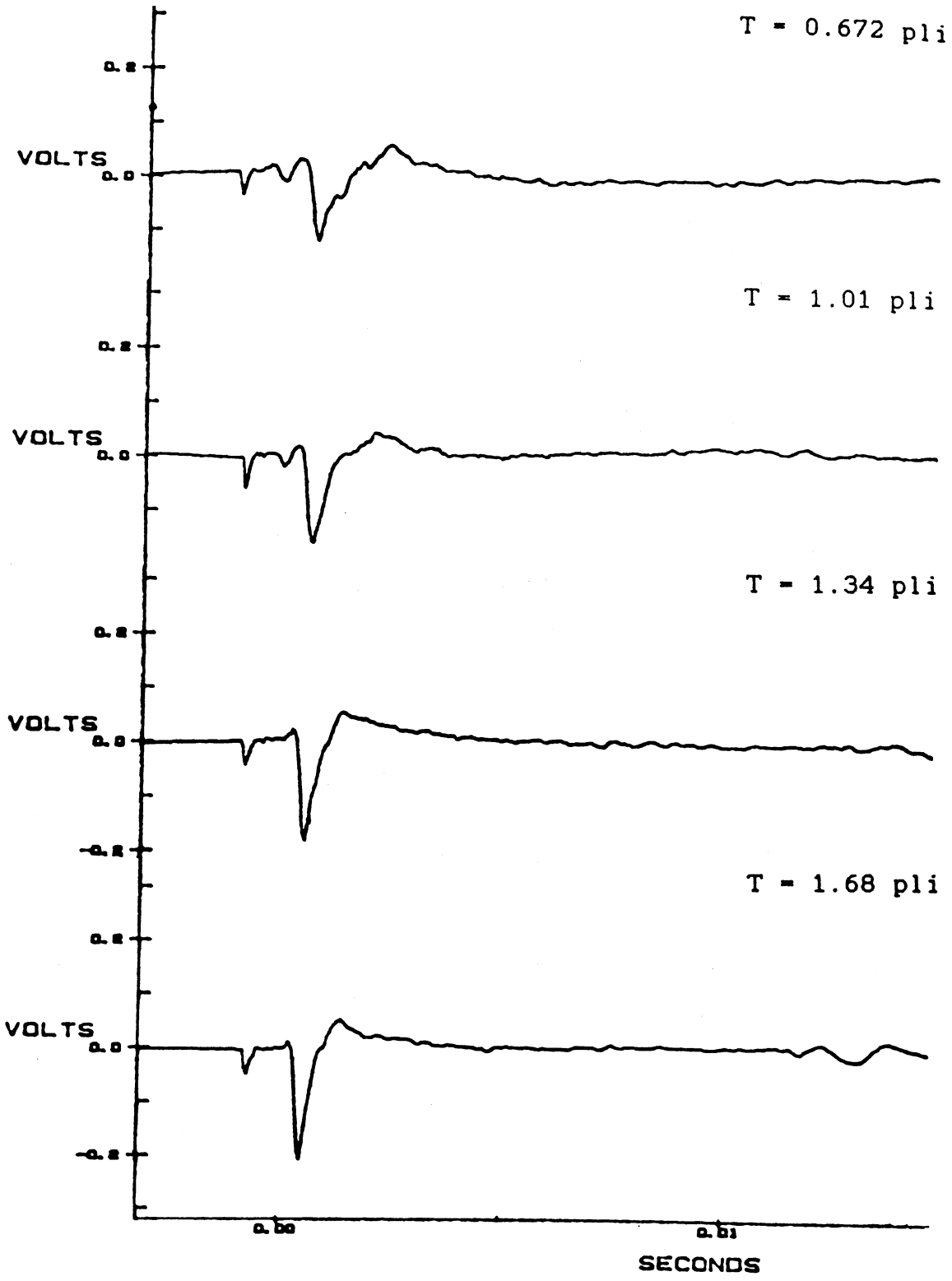

Figure 10. Variability in Wave Height and Width With Varying Tension on a Paper Web

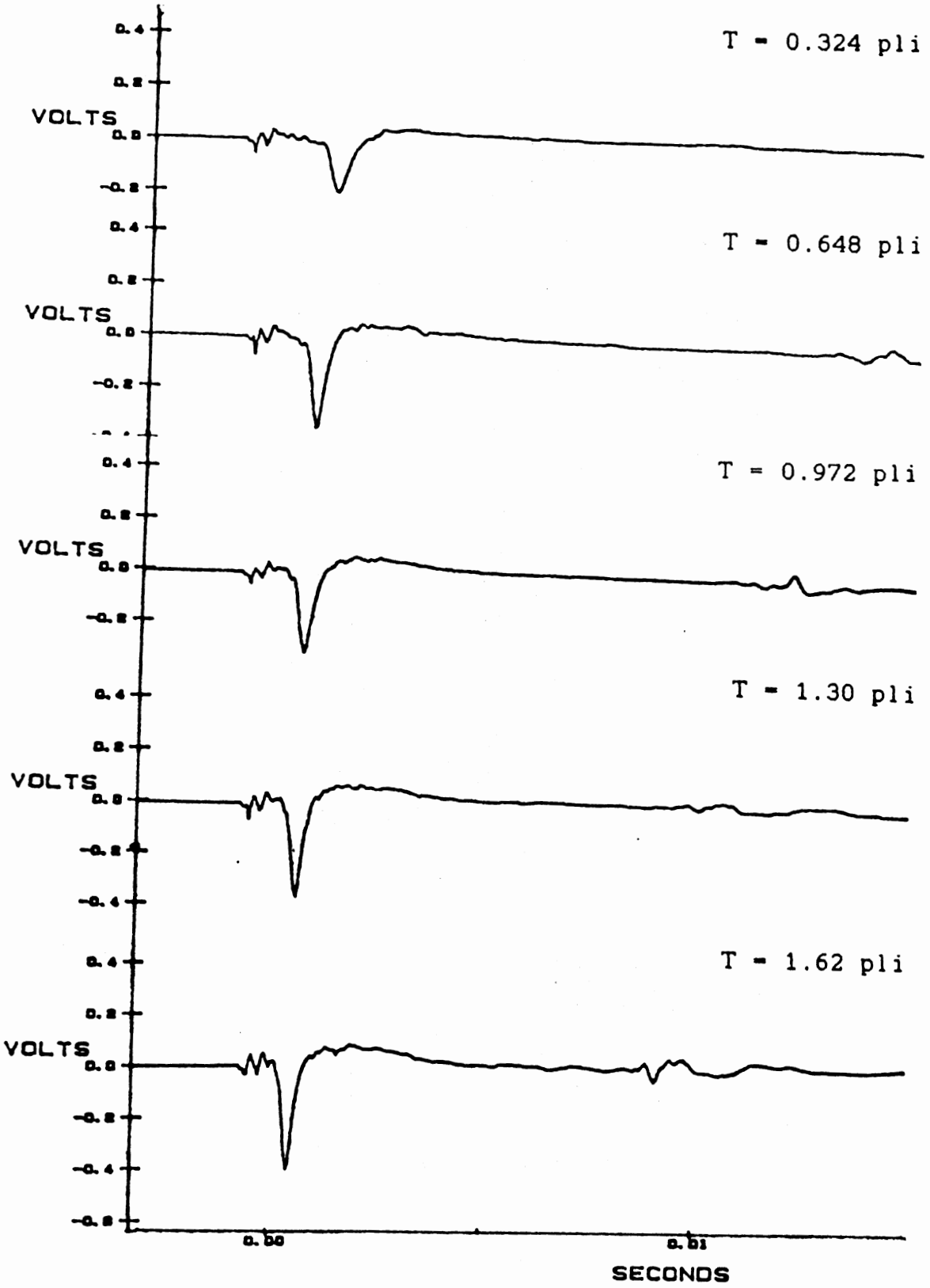

Figure 11. Variability in Wave Height and Width With Varying Tension on a Polypropylene Web

One can see that the pulse height is greater for the polypropylene web. The polypropylene, which is thinner and lighter than the paper, offers less impedance to the air pulse pressure than does the paper.

The next set of experiments was done using the revised pneumatic pulser, which was discussed in Chapter 5 and shown in Figure 5. The high-speed loop (from Figure 2) and traversing mechanism (from Figure 3) were also utilized. All of the signals produced by the pneumatic pulsers were less than 1 millisecond in duration, and the wave height of an unfiltered signal varied from about 100 to 400 millivolts, depending on the tension.

The first test was static, and the 6-inch paper web was used. The pressure going into the pulser was 80 psi. The microphone was placed 2 inches from the pulse source. The experiments were done for locations at 1, 2, 3, 4, and 5 inches from one web edge. The wave height and width were recorded from the digital oscilloscope for tensions of 0.663, 1.33, 1.99, 2.65, and 3.31 pli at each location. Unfiltered data were used.

The data are plotted in Tables I and II in the Appendix. Table I arranges the data so that a family of curves, wave height and width versus distance from web edge, is plotted for varying tensions. This family of curves is shown in Figure 12 for wave height and Figure 13 for wave width. Figure 12 clearly shows that, at all tensions, the maximum wave height occurs 2 inches from the web edge for

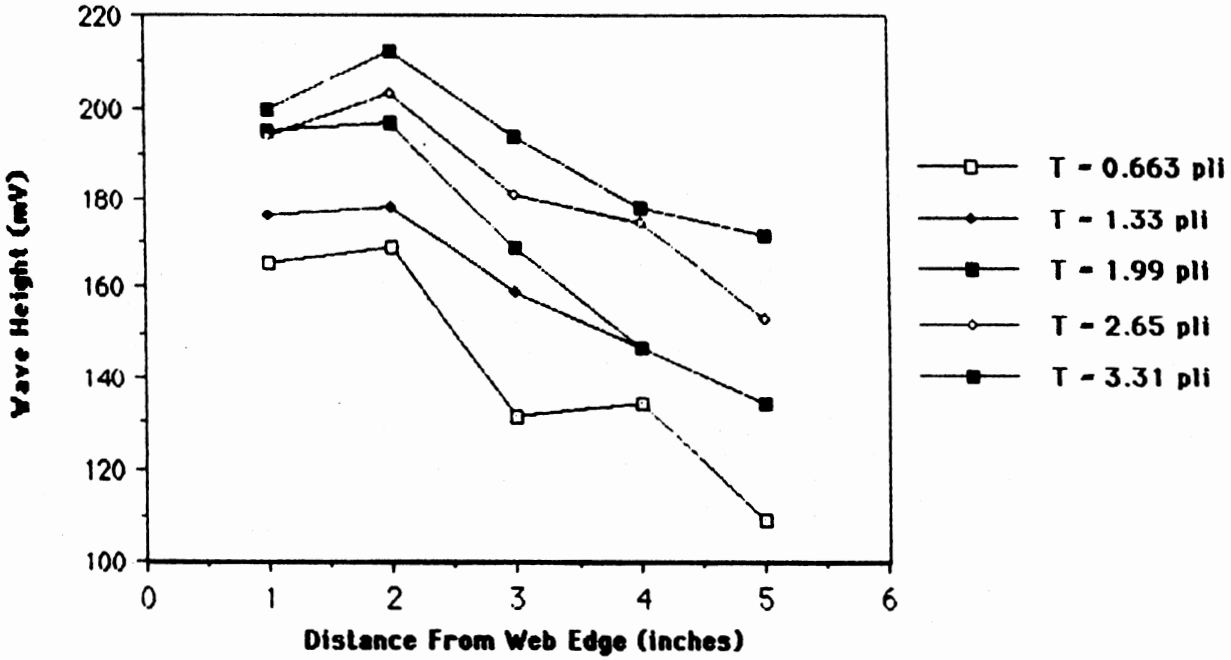

Figure 12. Wave Height Versus Distance From Web Edge for Different Values of Tension

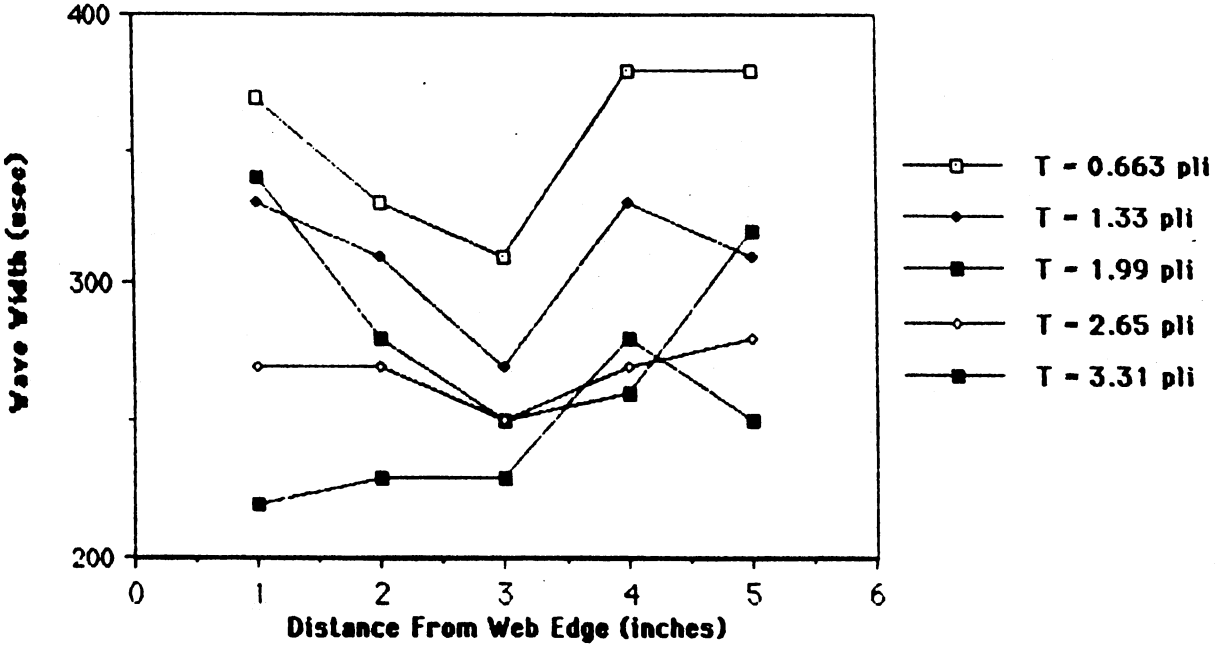

Figure 13. Wave Width Versus Distance From Web Edge for Different Values of Tension

this particular web. The maximum wave height of all the curves also corresponds to the maximum tension curve. Wave width, as shown in Figure 13, is a less reliable way of predicting tension than the wave height because the width is harder to measure. The data follow a less clear trend than those in Figure 12.

Table II arranges the data so that a family of curves, wave height and width versus tension, is plotted for varying distance from web edge. Figure 14 shows wave height versus tension curves at different locations across the web. Once again it can be seen that maximum tension occurs at 2 inches from the web edge for all tensions, and the maximum wave height of all the curves corresponds with the point 2 inches from the edge of the web. Also, a clear trend is observed that wave height increases with increasing tension for all the curves. Figure 15 shows wave width versus tension curves, and the wave width shows a generally decreasing trend with increasing tension. However, the data are less predictable for wave width than they are for wave height, and the wave width is a less reliable means of predicting tension than the wave height.

The next step in the experiments was to compare the averaged wave height among three samples at each tension taken from a static web and a dynamic web. Also, the change in the wave height among the three samples ($V_{max} - V_{min}$) was compared for the static and dynamic webs. The average wave heights and change in wave height are tabulated with tension

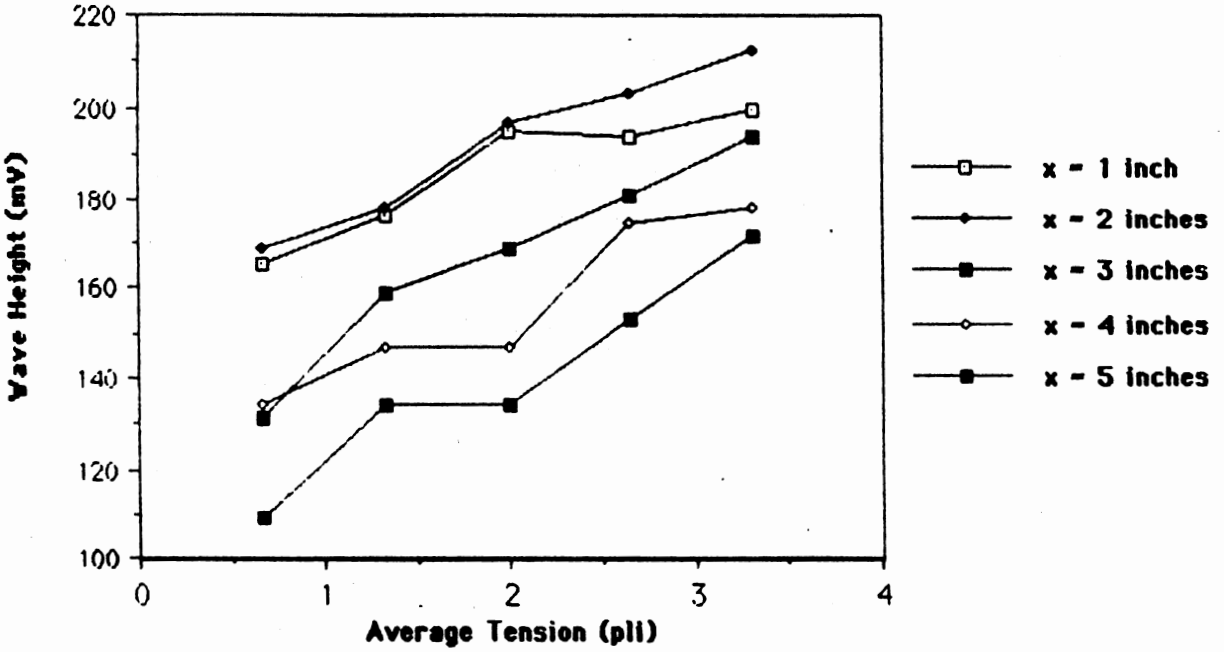

Figure 14. Wave Height Versus Tension at Different Locations From Web Edge

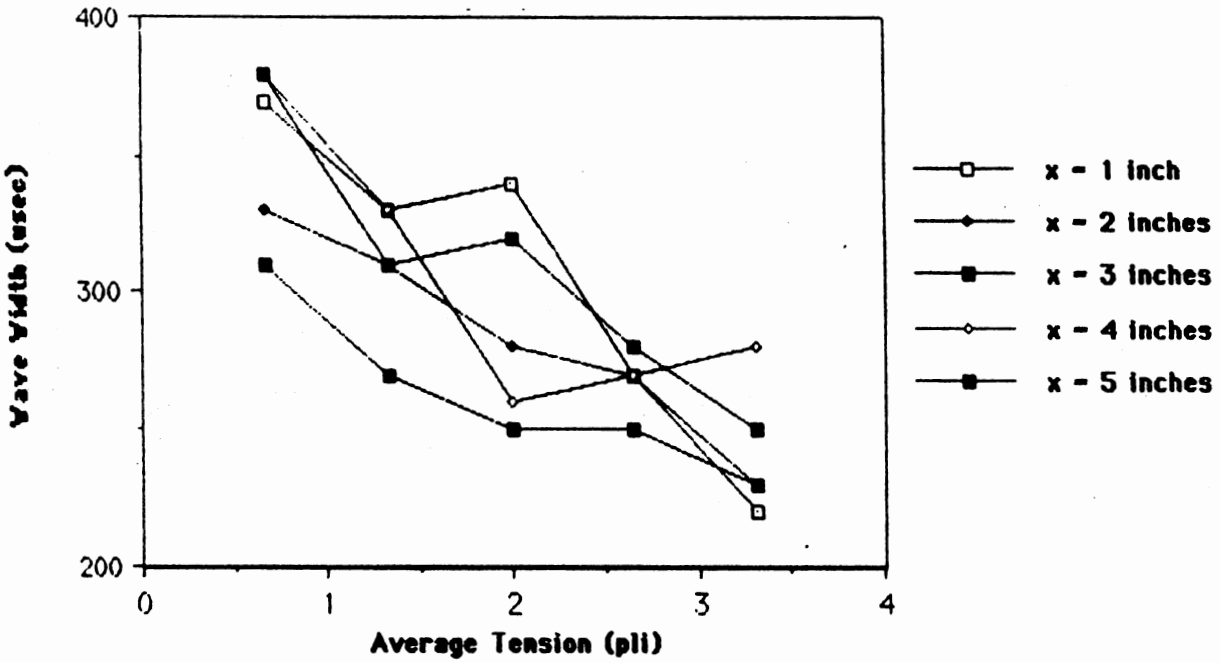

Figure 15. Wave Width Versus Tension at Different Locations From Web Edge

in Table III in the Appendix. The test was done using the updated pneumatic pulser at 70 psi, the high-speed loop, the traversing mechanism, and the 6-inch paper web. No filtering was utilized. The distance from the microphone to the web was about 0.07 inch. For the dynamic case, the web was run at about 400 feet per minute. The signal, which was picked up on the digital oscilloscope, was obtained from a microphone 2 inches from the pulse source.

Figure 16 shows the comparison of average wave heights for the two cases. As can be seen, the average wave height was substantially higher for the moving web as compared to the static web. This phenomenon could have occurred because the web was bouncing slightly, causing it to move closer to the pulser tube and increasing the interaction between the pulser tube and web.

Figure 17 shows the voltage variation ($V_{max} - V_{min}$) among the three samples versus average tension. As indicated by the figure, the pulse height varied much more on the moving web than on the static web. This variation could have been caused by the web bouncing slightly as it ran on the loop. The further the microphone was from the web, the weaker the signal would have been, and the wave height correspondingly would have been less.

It was suspected that the pulser tube, which was very close to the web, was interacting with the web in some way. For example, a nozzle-flapper displacement-to-pressure transducer utilizes the principle of a fixed flow

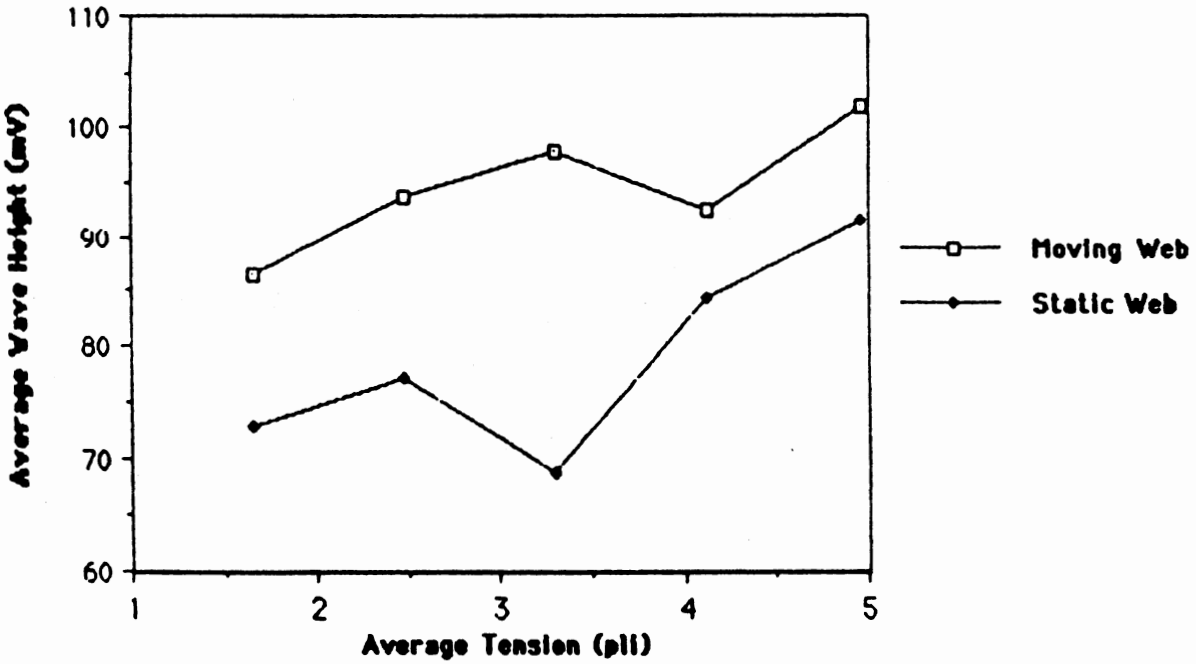

Figure 16. Comparison of Average Wave Heights for Static and Moving Webs

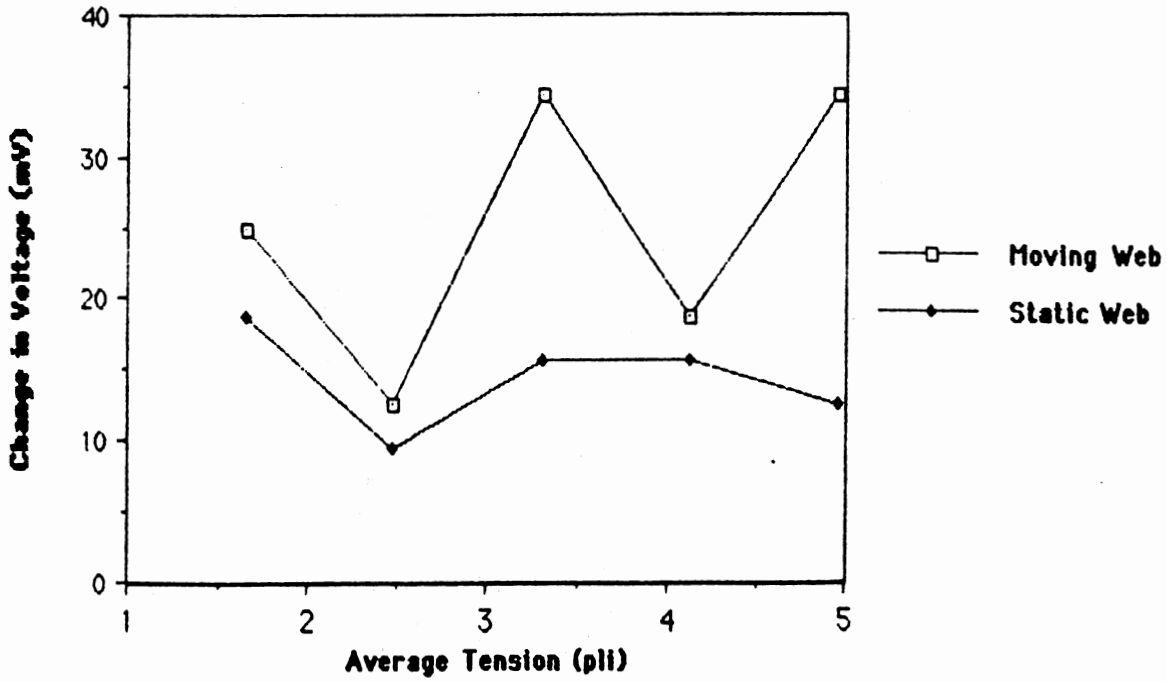

Figure 17. Voltage Variation (V_{max} - V_{min}) Among Three Samples Versus Average Tension

restriction and a variable flow restriction (13). The variable flow restriction, or "flapper," is adjusted to change the distance x_o, causing a change in output pressure p_o. For a limited range of motion, p_o is nearly proportional to x_o and is extremely sensitive to it. Therefore, the pulse height variation with pulser tube distance from the web was investigated.

The revised pneumatic pulser at 80 psi, the 6-inch paper web, the traversing mechanism, and the high-speed loop were again utilized. The test was done statically at two different places on the web for comparison purposes. The data were unfiltered. The distance between the microphone, which was 2 inches from the pulse source, and web was measured using feeler gauges.

Table IV in the Appendix tabulates the data for wave height at two different places in the web along with pulser tube distance from the web. These data are plotted in Figure 18. No clear-cut trend exists for the two samples; however, the pulser tube distance from the web does have an effect on the pulse height. Also, as for the nozzle-flapper transducer case, the linear range is probably very small, and a great number of samples would be required to locate the linear region. Also, a more accurate means of measuring the distance from the tube to the web would be required.

The next concern was to find how the wave varied with supply pressure into the pulser. The original pneumatic pulser with 1/4-inch-OD plastic tubing was utilized. The

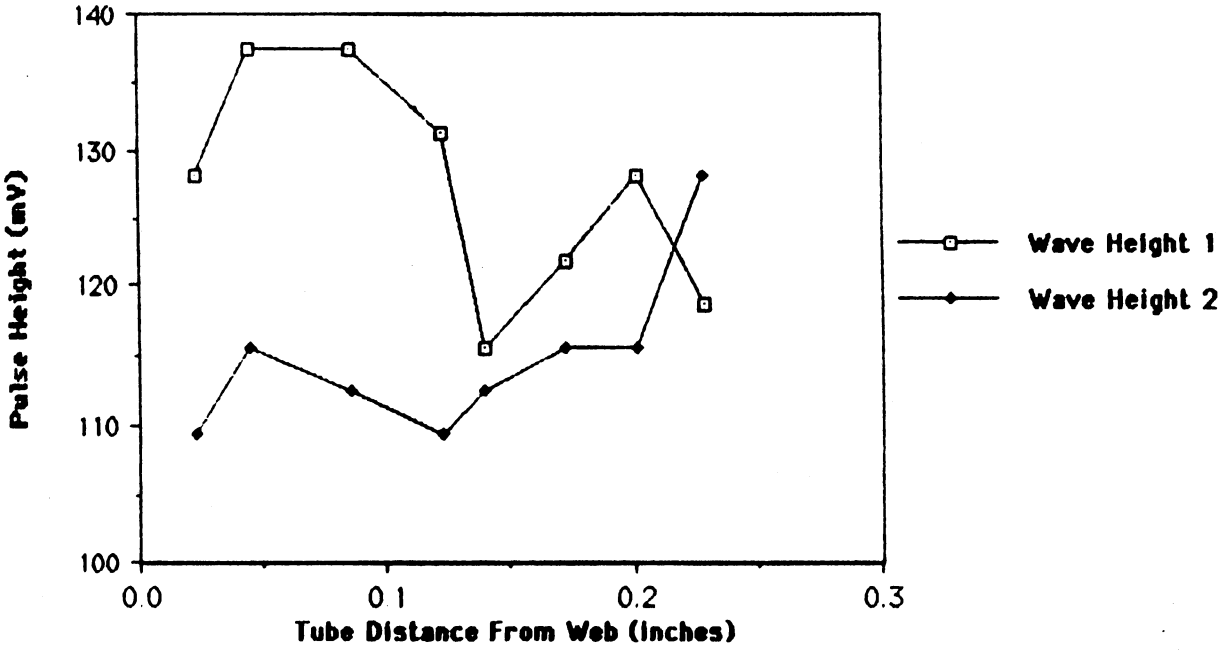

Figure 18. Pulse Height Versus Pulser Tube Distance From Web

tension was set at 2.81 pli on the 6-inch paper web. The test was done statically using unfiltered data, and the distance from the pulser tube to the web was about 0.1 inch.

The pressure and wave height data are tabulated in Table V in the Appendix. The data are plotted in Figure 19. As is seen from the figure, the wave height consistently increases with increasing pressure input into the pulser mechanism. The increase in wave height is about 300 millivolts with a 60-psi pressure increase. Therefore, a consistently high pressure level is important to the consistent properties of the wave.

Since the experiments concerning measurement of time delay utilize two microphones, the wave heights of two microphones, one 2 inches downstream of the source and one 4 inches downstream of the source, were compared. The original pneumatic pulser was utilized, with an input pressure of about 115 psi and 1/4-inch plastic tubing. The distance between the pulser tube and the web was about 0.1 inch. The test was done statically, and the 6-inch paper web was used. Unfiltered data were again used.

The data are shown in Table VI in the Appendix. These data are plotted in Figure 20. The wave height recorded by the microphone 4 inches from the source was always larger than that recorded by the microphone nearer to the source. This occurrence may have been due to the fact that the second microphone was more sensitive than the first microphone. However, the waves followed almost the same

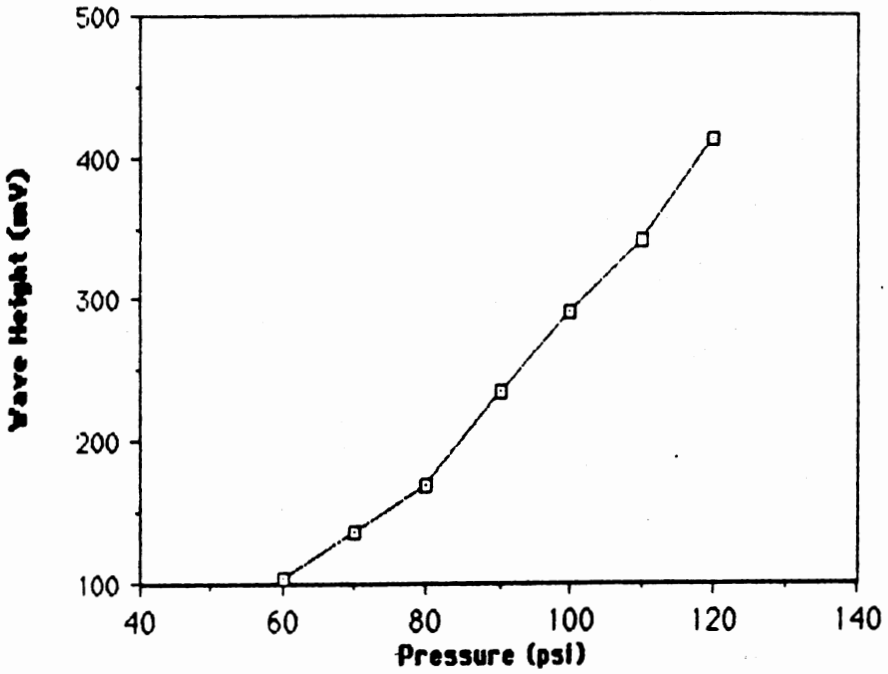

Figure 19. Wave Height Variation With Pressure

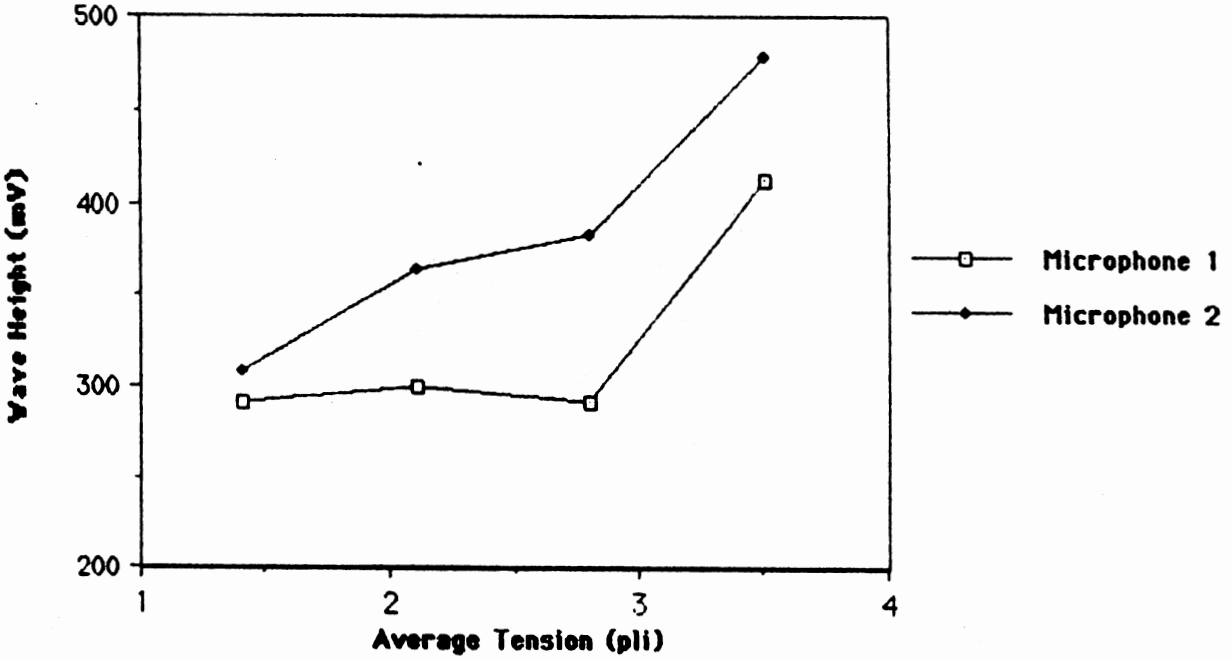

Figure 20. Comparison of Wave Height for Two Microphones Versus Average Tension

trend with increasing tension. Therefore, the difference in the two wave heights would not cause a problem.

A profile of wave variation with distance from web edge was also done for the two wave heights. The original pneumatic pulser with 120-psi pressure and 1/4-inch-OD plastic tubing was again utilized, along with the 6-inch paper web. The tension was 2.81 pli in the web, and the test was done statically.

The data are shown in Table VII in the Appendix and are plotted in Figure 21. The wave height profiles are almost the same for both microphones; the maximum wave height occurs at 2 inches from the web edge, and the edges of the web have the lowest wave heights. However, as can be seen, the second downstream microphone had a more dramatic wave height decrease between 3 and 4 inches from the web edge than the first downstream microphone did. However, this occurrence should not constitute a problem.

A high-pass filter circuit was used on the data for the following experiment. Average wave height from three different samples, as well as change in wave height among the samples, was determined for varying tensions. The test was done dynamically, at about 550 feet per minute. The original pneumatic pulser, with 1/4-inch-OD plastic tubing and 120-psi supply pressure, was also used, as was the 6-inch paper web.

Table VIII in the Appendix tabulates the data for tension, average wave height, change in wave height, and

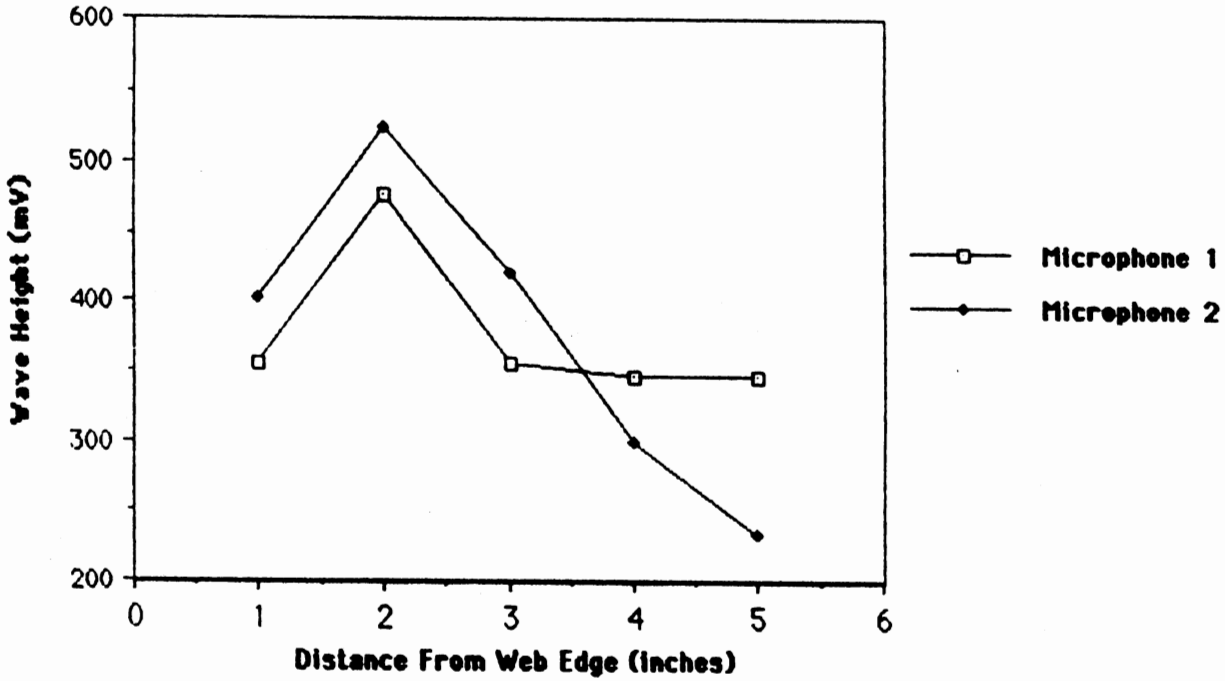

Figure 21. Comparison of Wave Height for Two Microphones Versus Distance From Web Edge

maximum and minimum heights. Figure 22 shows the average wave height versus tension plot. As expected, the filtered data show the same trend as the unfiltered data--increasing wave height with increasing tension. The only difference is that the wave height varies more because of the circuit gain. Figure 23 shows the variation in wave height (V_{max} - V_{min}) versus tension plot. The change in voltage shows the same "zigzag" trend as the change for the unfiltered data for a dynamic web, shown in Figure 17.

Cross-Correlation Tests

The cross-correlation of some signals was taken to determine the difficulty of obtaining time differences by this method.

A static experiment was done using the 6-inch aluminized web, in which the Precision Diode Circuit was used to eliminate voltages below zero. The original pneumatic pulser was used with a supply pressure of 120 psi.

A sample of the original data, at a tension of 1.49 pli, is shown in Figure 24. The cross-correlation of the two waves, which was done by the Fourier analyzer, is shown in Figure 25. As is seen from the figure, some large negative spikes exist in the cross-correlation. These negative spikes are caused by a very small negative portion in the second acoustic wave in Figure 24, caused by an offset in the circuit. When this negative portion

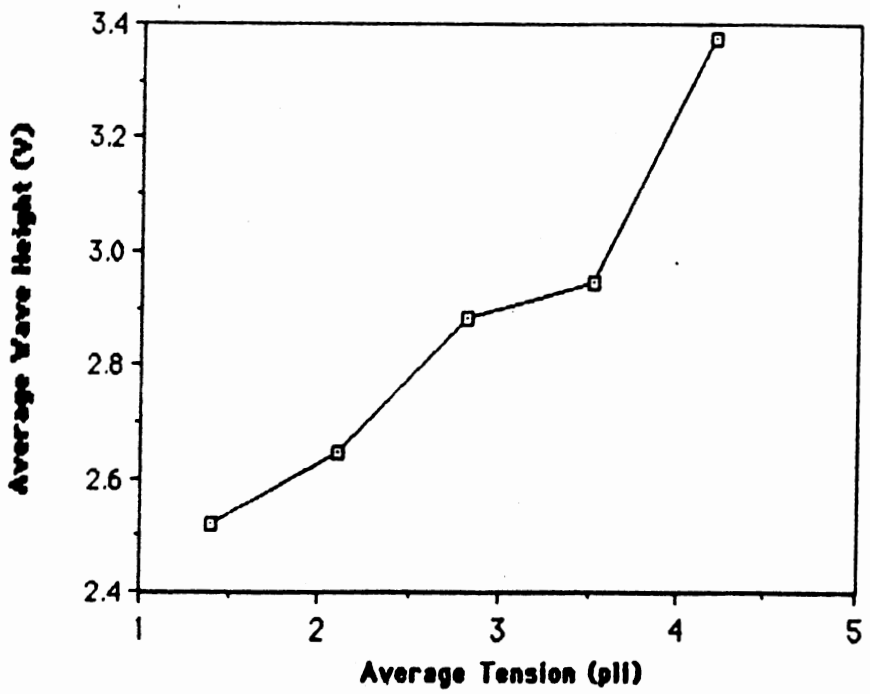

Figure 22. Average Wave Height Versus Tension Using High-Pass-Filter Data

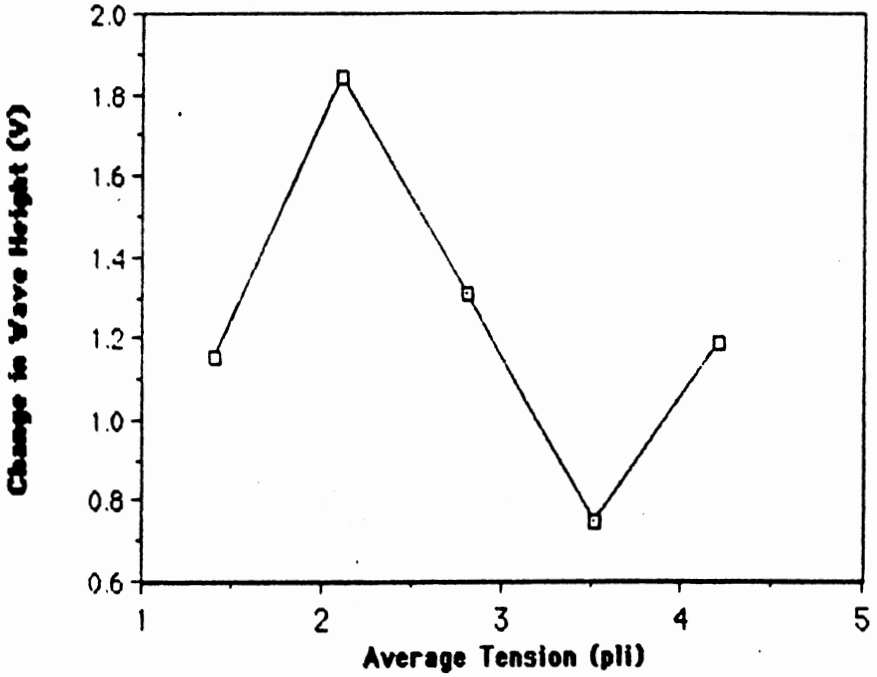

Figure 23. Wave Height Variation (V_{max} - V_{min}) Versus Average Tension for Filtered Data

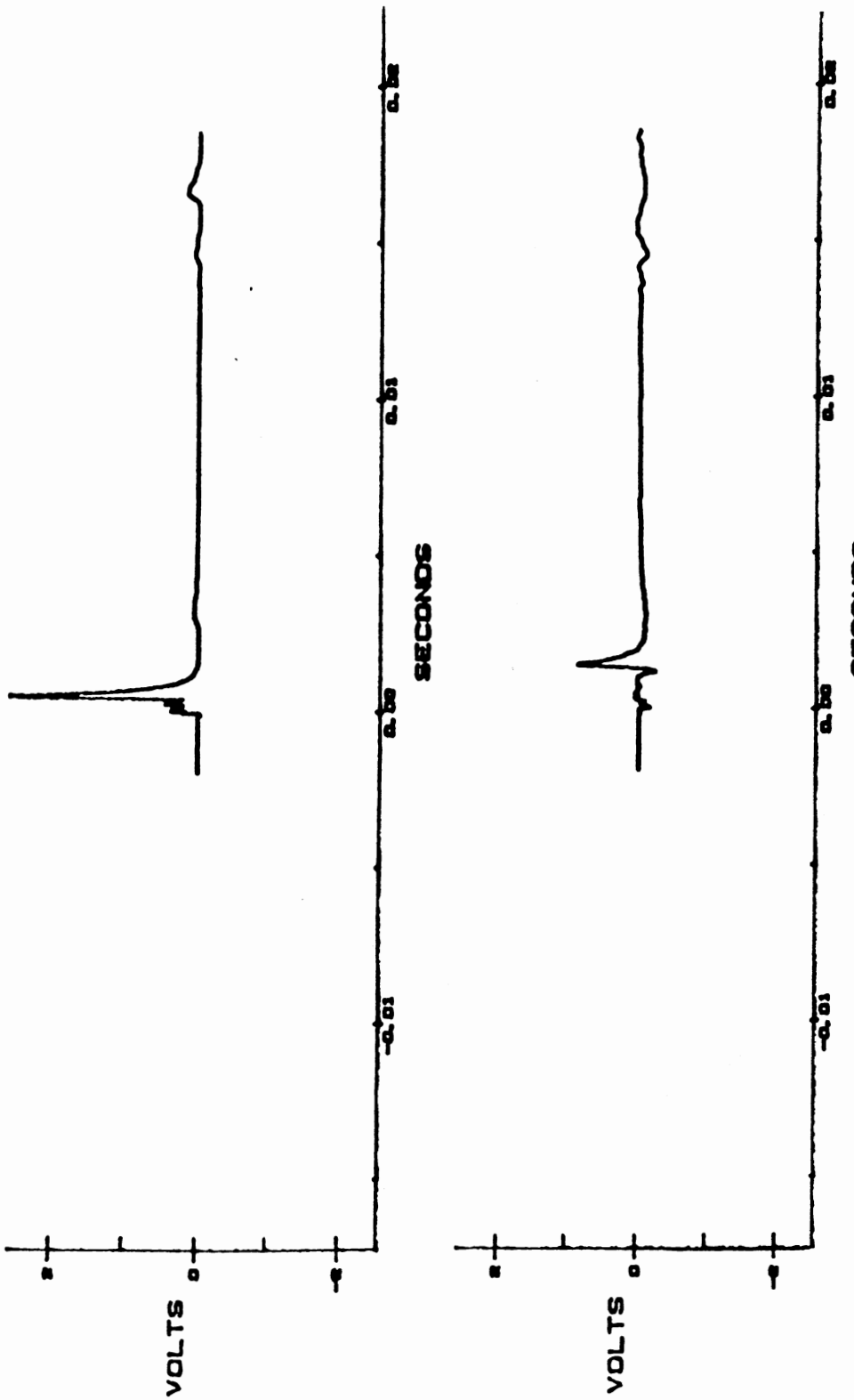

Figure 24. Precision Diode Circuit Samples

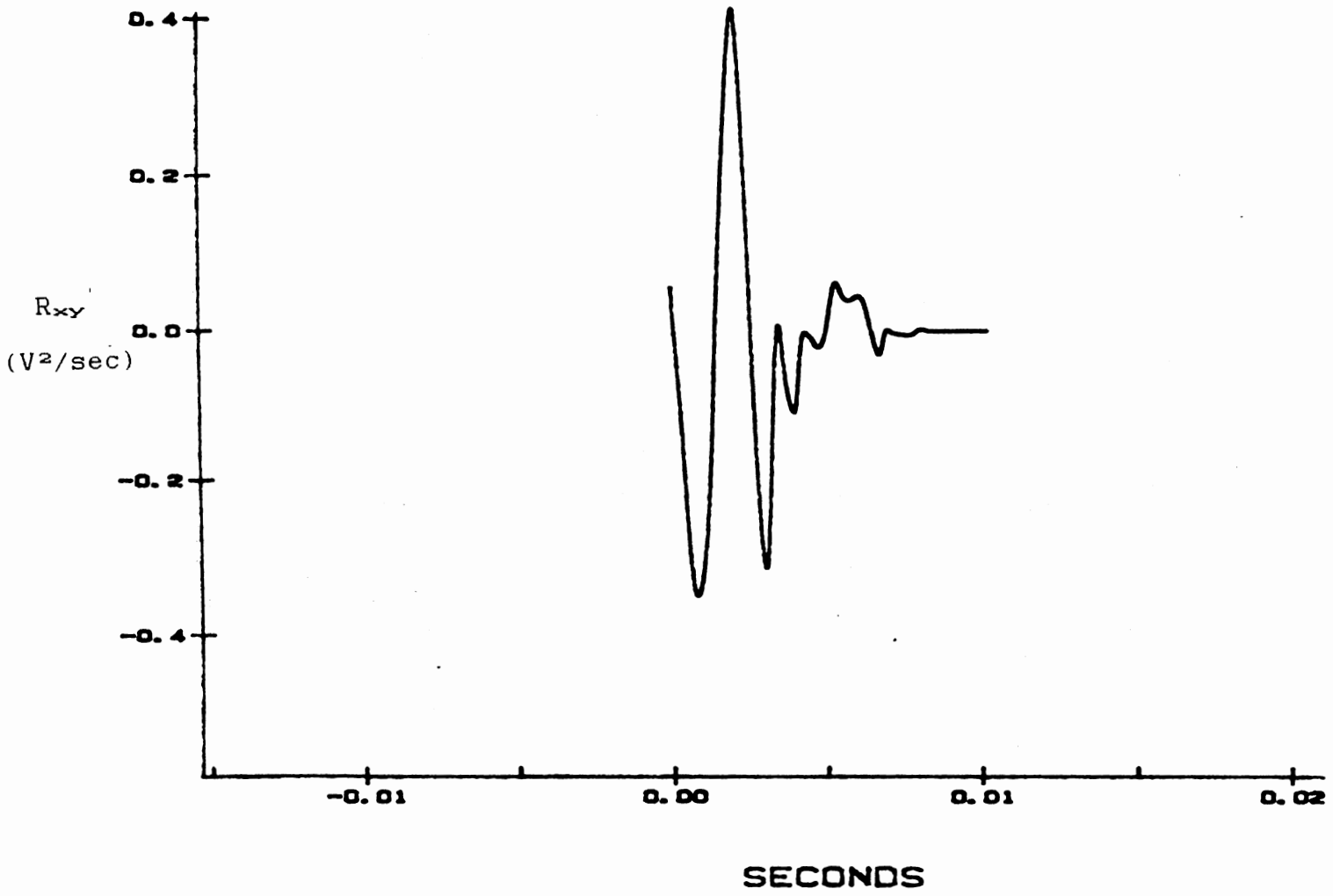

Figure 25. Cross-Correlation of Precision Diode Circuit Samples

correlates with the sharp, tall part of the first acoustic wave, a big negative spike is the result.

Also, when the small areas of noise in front of the web signals correlate, several spikes are produced in the cross-correlation. Thus it is difficult to determine which spikes are the actual web signal correlation by which the time difference can be determined.

Another potential problem is the fact that, as the tension increases, these spikes come closer together to one another, making them indistinguishable from each other in some cases. At a tension of 2.24 pli, this phenomenon is observed.

A cross-correlation was done by hand using approximate acoustic waves. The wave heights used were 3.2 volts and 1.0 volt for the first and second downstream microphones, respectively. The waves were digitized by hand and the cross-correlations computed. Figure 26 shows this approximate cross-correlation. If the actual signal had no noise at the beginning of it, the cross-correlation would resemble this figure. The maximum value of the cross-correlation, which occurs at the time of the delay between the two original signals, is about 40.000 square millivolts per second, or 0.04 square volts per second.

The cross-correlation is not recommended for use with this signal because of the above-mentioned problems. A rough cross-correlation would be a possibility; however, for the purposes of determining time differences, the original

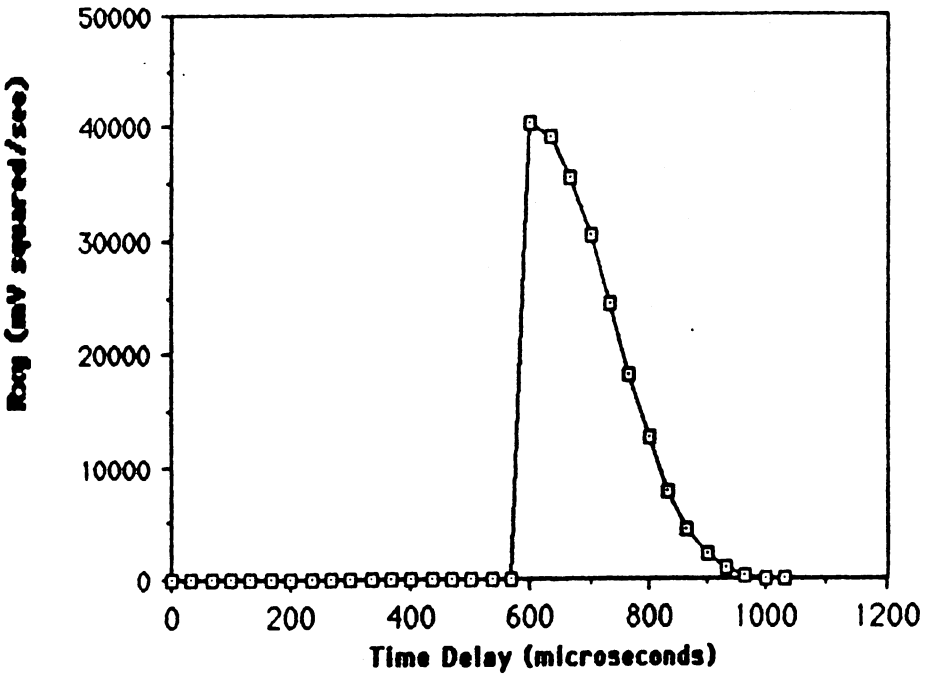

Figure 26. Hand Cross-Correlation Versus Time Delay

signal is much better because it is much cleaner than the cross-correlation. At high tensions, the sampling device would need to have a very high sampling rate so that the peaks of the cross-correlation would be spread out and thus distinguishable.

Tension Distribution Tests

The ultimate purpose of these tests was to determine how close the average of the tension distribution was to the known average tension. However, as explained in Chapter III, in order to use the tension equation for an air-loaded web, the wave number must first be known. Since the wave number depends on frequency, a wave frequency must be estimated.

The first step was to see how closely the wave speed obtained from experimentation matched the wave speed from the formulas (8) in Chapter II, Literature Review, as well as $(T/\rho)^{1/2}$. The wave frequency had to be estimated for these formulas. A battery of static tests was done in which the wave width was estimated for both microphones for tensions varying from 0.746 to 3.73 pli on a 6-inch paper web. Considering the wave to be half of a sinusoidal wave, one could estimate the frequency to be double the reciprocal of the wave width--i.e., the reciprocal of the wave period. Wave speed could then be calculated using the formulas. The results of these calculations, as well as $(T/\rho)^{1/2}$, are shown in Table IX in the Appendix. The data are tabulated

in Figure 27 for the first microphone and Figure 28 for the second microphone. These figures show that, for both microphones, the wave speed determined from the time difference is close to the results from the air-loaded web formulas--much closer than $(T/\rho)^{1/2}$, especially for high tensions. However, the experimental wave speeds were consistently higher than the wave speeds produced by the air-loaded web equations.

One does not want to determine the frequency at each tension. Therefore, the next step was to determine how close the results would be if an averaged frequency over the tension range was used. The frequency for the first microphone, which was averaged over the tension range 0.746 to 3.73 pli, turned out to be 1485 hertz. This frequency was used in the air-loaded web equations to determine if any considerable difference could be noted. The results of these calculations are tabulated in Table X in the Appendix and are shown in Figure 29. As is seen from the figure, no notable difference exists between the variable- and average-frequency wave speed results. The deviations were all less than 2 percent. Therefore, the constant frequency could safely be used.

Next the tension profile experiments were done utilizing the traversing mechanism on the high-speed loop. The test was done statically using the original pneumatic pulser with 1/4-inch-OD tubing and a 120-psi supply pressure. The 6-inch aluminized web was used. Six samples

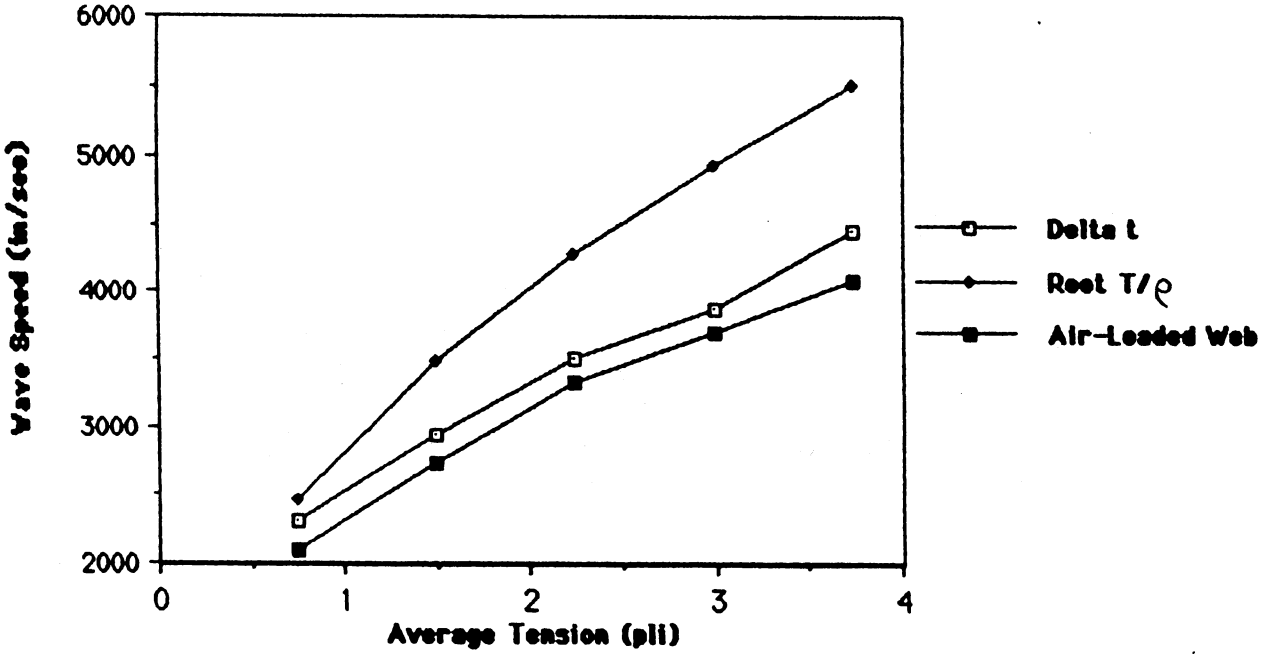

Figure 27. Wave Speed Versus Average Tension for Microphone 1

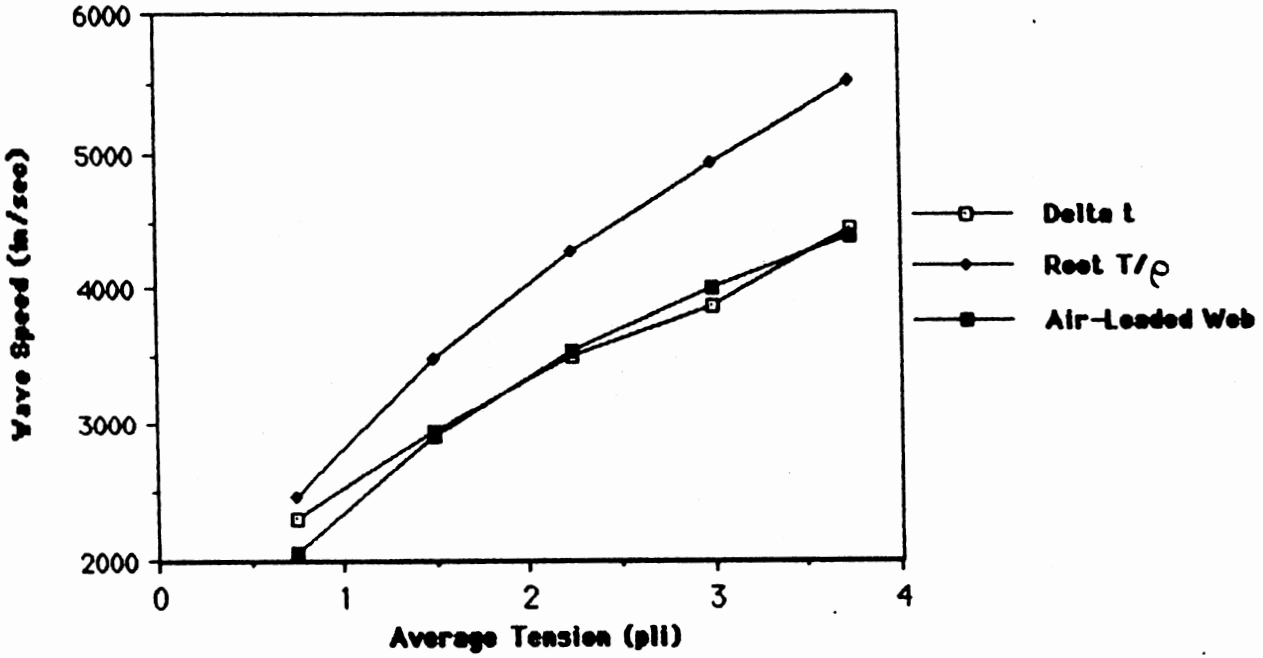

Figure 28. Wave Speed Versus Average Tension for Microphone 2

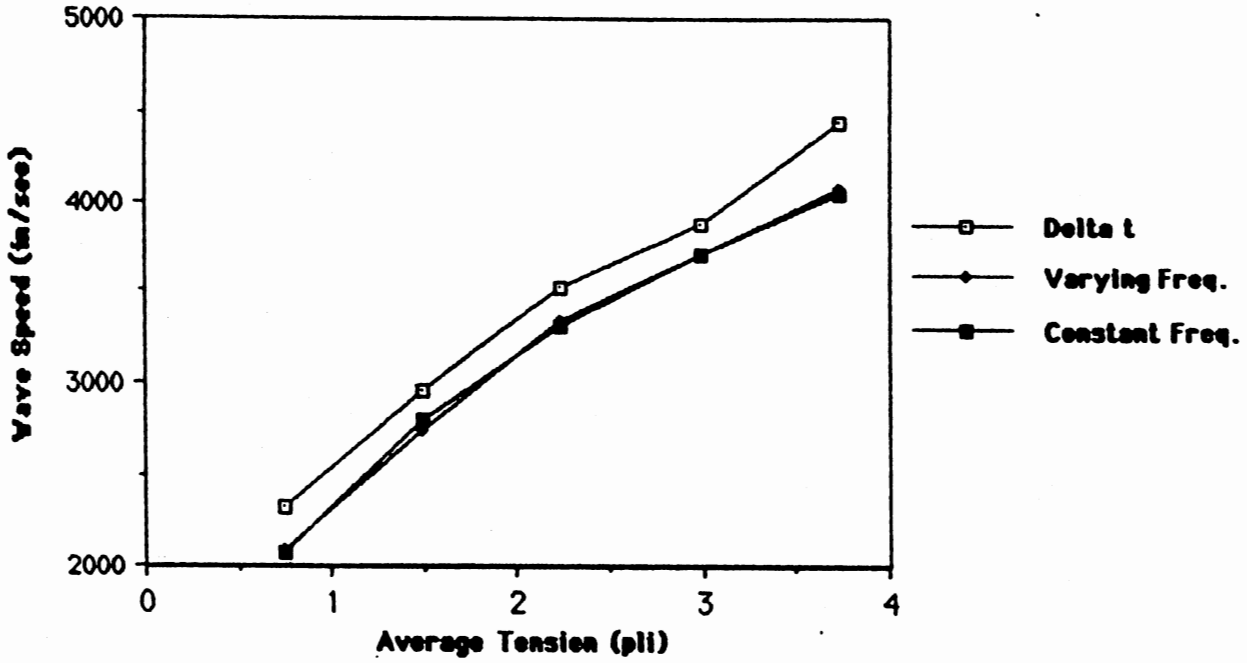

Figure 29. Wave Speed Versus Average Tension for Varying and Constant Frequency

were taken across the web, and four tensions were applied at each location. The digital oscilloscope was used to read time differences. The results of this experiment are tabulated in Table XI in the Appendix.

The equation

$$V_{ph} = \left[\frac{T}{\rho_w + \frac{2 * \rho}{(K^2 - k^2)^{1/2}}} \right]^{1/2}$$

where T is the tension, ρ_w is the areal density of the web, ρ is the density of the air, K is the wave number for the web in air, and k is the wave number for the air, gives the same results for phase velocity as the previously mentioned equations. This equation can be rearranged to solve for tension and put into a computer program to directly solve for tension. Utilizing the wave speed results of the tension profile experiment and the above-determined frequency to calculate the wave number, the tension can be calculated at each location on the web. These calculations are then averaged so that they can be compared with the known average tension. The results are tabulated in Table XII in the Appendix. Figure 30 is a graph of the results.

From the figure, it can be observed that the average of the tension profile is always greater than the known average tension. However, the error is consistent. Some possible sources of error will now be discussed.

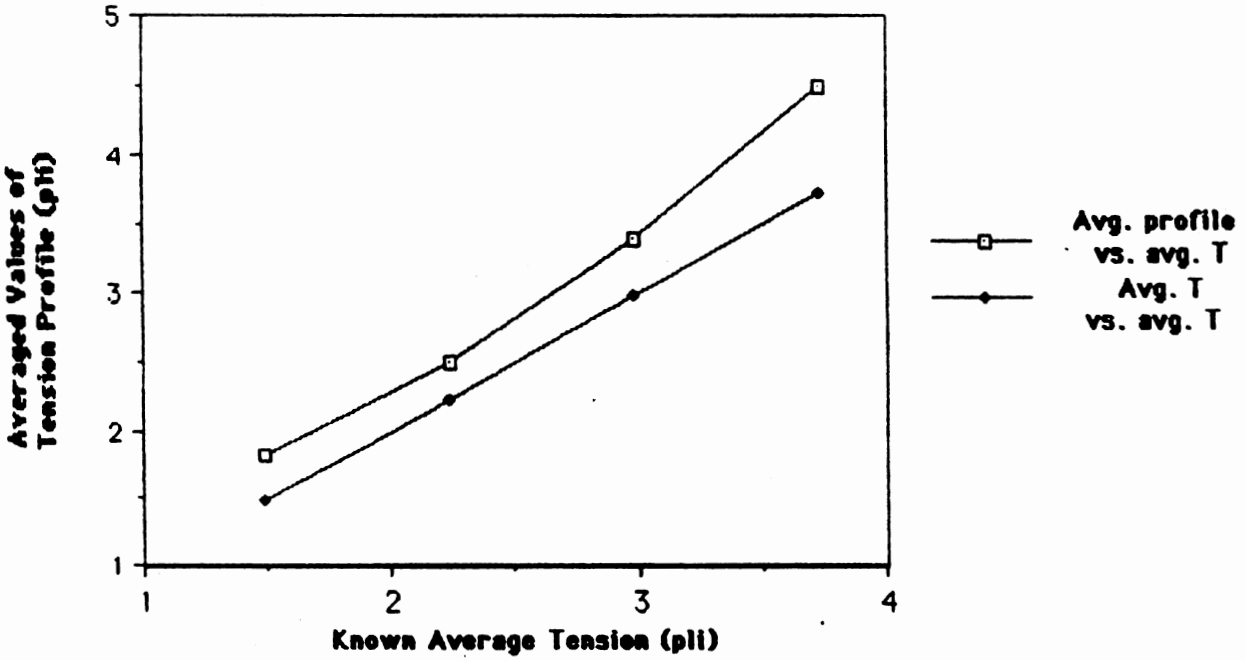

Figure 30. Comparison of Averaged Tension Profile With Known Average Tension

The error could be partially due to the approximation of the frequency used in the wave speed formulas, which may have caused the experimental wave speed to be consistently higher than the calculated wave speed. The inconsistency could also be due to an error in the static model of the high-speed loop. The model of the load cell involved some measurement of angles, which was almost certainly a source of error. From the static model, the tension equation in pounds per linear inch was determined to be

$$T = \frac{\text{weight}}{(\tan \theta_1)(\cos \theta_2 + \cos \theta_3)(\text{width})}$$

A propagating error analysis (14) was done on this equation using the relationship

$$u_T = \left| u_{weight} \frac{\partial T}{\partial (weight)} \right| + \left| u_{\theta 1} \frac{\partial T}{\partial \theta_1} \right| + \left| u_{\theta 2} \frac{\partial T}{\partial \theta_2} \right|$$

$$+ \left| u_{\theta 3} \frac{\partial T}{\partial \theta_3} \right| + \left| u_{width} \frac{\partial T}{\partial (width)} \right|$$

The uncertainties u were estimated to be: 1 percent for weight, 1 percent for width, 2 percent for θ_1, 3 percent for θ_2, and 5 percent for θ_3, which was the hardest angle to measure. The propagating error analysis led to an overall error of 5 percent.

Another source of error may have been the time difference measurements from the digital oscilloscope. Although the instrument has a fine setting for measuring

voltage differences, only a coarse setting is available for measuring time differences. Therefore, it is difficult to get the cursor exactly on the peak of the signal. Also, human limitations may be a hindrance in getting the cursor on the peak.

All of these errors combined were probably enough to cause a considerable change in the tension comparisons.

Static Versus Dynamic Tests

Dynamic tests had to be handled in a different manner than static tests, because the speed of the web affected the speed of sound in the web. For a static test, the speed of sound in the web was easily handled; c_w, the speed of sound in the web, was equal to the distance between microphones, x, divided by the time difference between the two signals, delta t. The case of a dynamic web with two microphones downstream of the signal will now be discussed.

Let c_A be the speed of sound in air, c_w be the speed of sound in the web, and V_w be the speed of the web. The air spike travels so fast that one can assume it reaches both microphones at the same time. Let t_1 and t_2 be the time differences between the air spike and the web signal for Microphones 1 and 2, respectively. For Microphones 1 and 2, the time to the air pulse, t_A, is equal to x/c_A, where x is the distance from the pulser to the first microphone. The distance to the web pulse, t_w, is $x/(V_w + c_w)$ for the first microphone, where x is the distance from pulser to

Microphone 1. For equal spacing from pulser to Microphone 1 and Microphone 1 to Microphone 2, t_w is $2x/(V_w + c_w)$ for Microphone 2.

Now one can figure t_1 and t_2 as $t_w - t_A$ for both microphones and subtract t_1 from t_2, obtaining the expression

$$t_2 - t_1 = \frac{x}{V_w + c_w}$$

Solving this expression for c_w yields

$$c_w = \frac{x}{t_2 - t_1} - V_w$$

which can be utilized to find speed of sound in the web.

Another microphone setup was used to cancel web speed out of the expression for speed of sound in the web. One microphone was placed upstream of the pulser, and the other was placed downstream of the pulser at an equal distance. The expression is derived as follows.

Let t_1 be the time to the web pulse of Microphone 1, which is downstream of the pulser, and t_2 be the time to the web pulse of Microphone 2, upstream of the pulser. Then we can write

$$t_1 = \frac{x}{c_w + V_w} \qquad \text{and} \qquad t_2 = \frac{x}{c_w - V_w}$$

Both of these expressions can be solved for V_w, web velocity, and set equal to each other. Doing so yields

$$\frac{x - (c_w * t_1)}{t_1} = \frac{-x + (c_w * t_2)}{t_2}$$

Rearranging this equation to solve for c_w yields

$$c_w = \frac{x}{2 * t_1} + \frac{x}{2 * t_2}$$

This expression can be used to solve for speed of sound in the web.

Repeatability of Experiments

A set of experiments was repeated for the purpose of determining the repeatability of results. The experiments consisted of recording time distances between two waves at five locations across the web width and using the air-loaded web formulas to determine tensions from the time differences. The original pneumatic pulser was used for these experiments, with 1/4-inch-OD plastic tubing and inlet pressure of 120 psi. The test was done statically on a 6-inch paper web. The average applied web tension was determined to be 2.81 pli. No filtering was used on the data, and the distance between the pulser tube and web was about 0.1 inch. Time delays were read from the digital oscilloscope. A sample of the waveforms is shown in Figure 31.

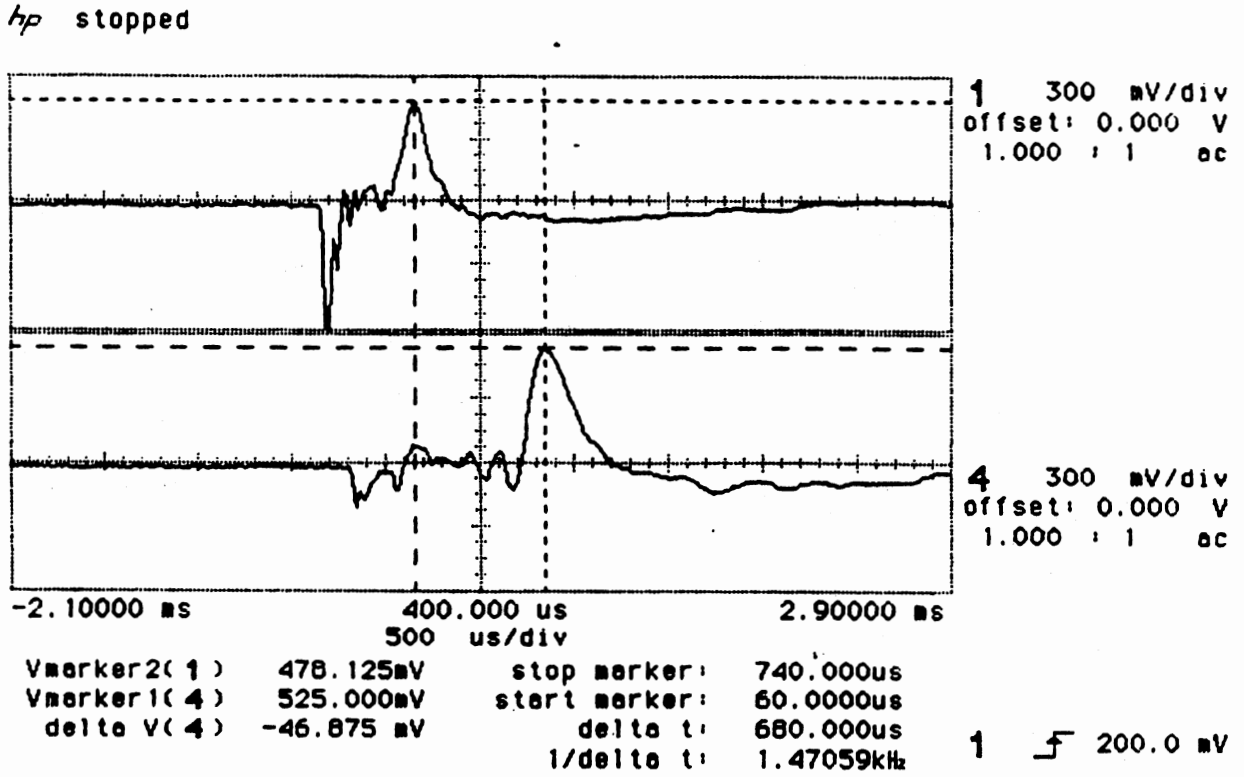

Figure 31. Waveform Samples Used to Obtain Time Delays

The results of the experiments are shown in Table XIII in the Appendix and are plotted in Figure 32. The tensions for both experiments follow the same trend across the web, but the differences in time delay range from 3.0 to 8.9 percent. Since the test involved moving the traverse, one reason for this error could be that, for the repeated experiment, the traverse was not moved to exactly the same spot as it was in the original experiment. The tension would change and, therefore, the time difference would change. Also, since the wave changed very slightly in shape with each air pulse, the peak could have moved slightly. The limitations of time delay measurements with the digital oscilloscope, as discussed previously, are also a factor.

Comparison of Waveforms

Each of the signal generation and processing methods generated quite a different signal. The shapes and problems with these signals will now be discussed.

The filtered signal from the revised pneumatic pulser with an inlet pressure of about 55 psi is shown in Figure 33. This signal was recorded in a 6-inch paper web at an applied average tension of 1.03 pli. The time difference between the two signals, from peak to peak, is 1080 microseconds. The test was done statically.

The above signal was fed into the Schmitt trigger, which remains high until 1.6 volts, when it shuts off. It remains off until the voltage is 0.8 volts and then turns

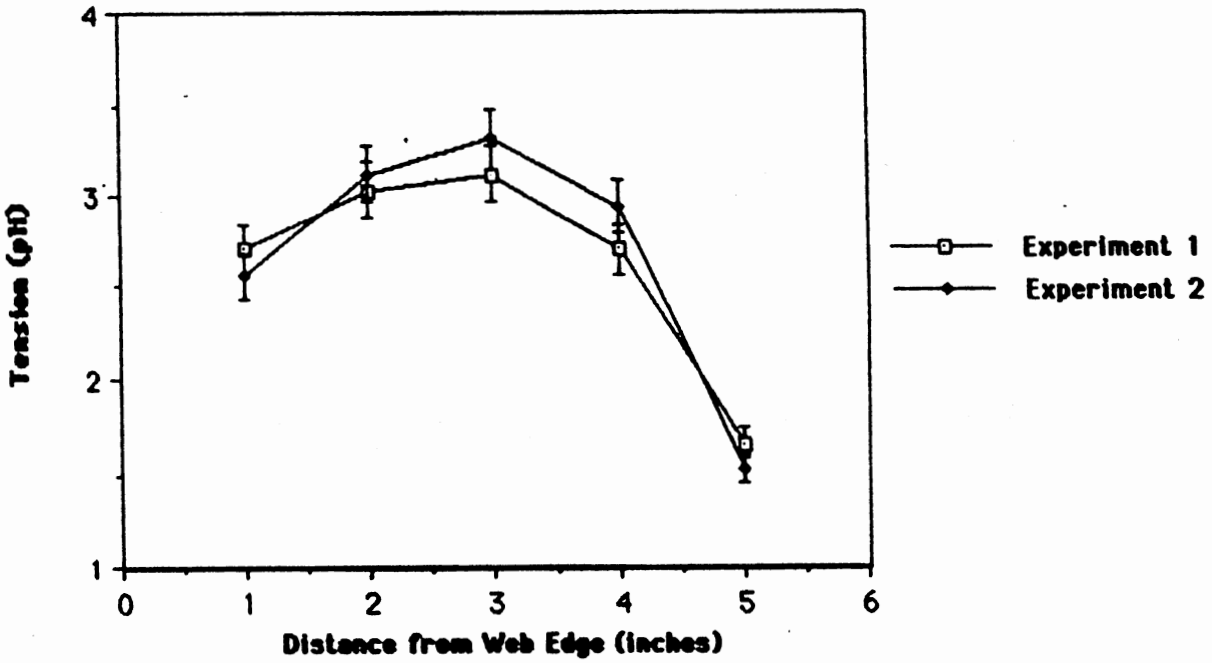

Figure 32. Comparison of Tension for Two Experiments

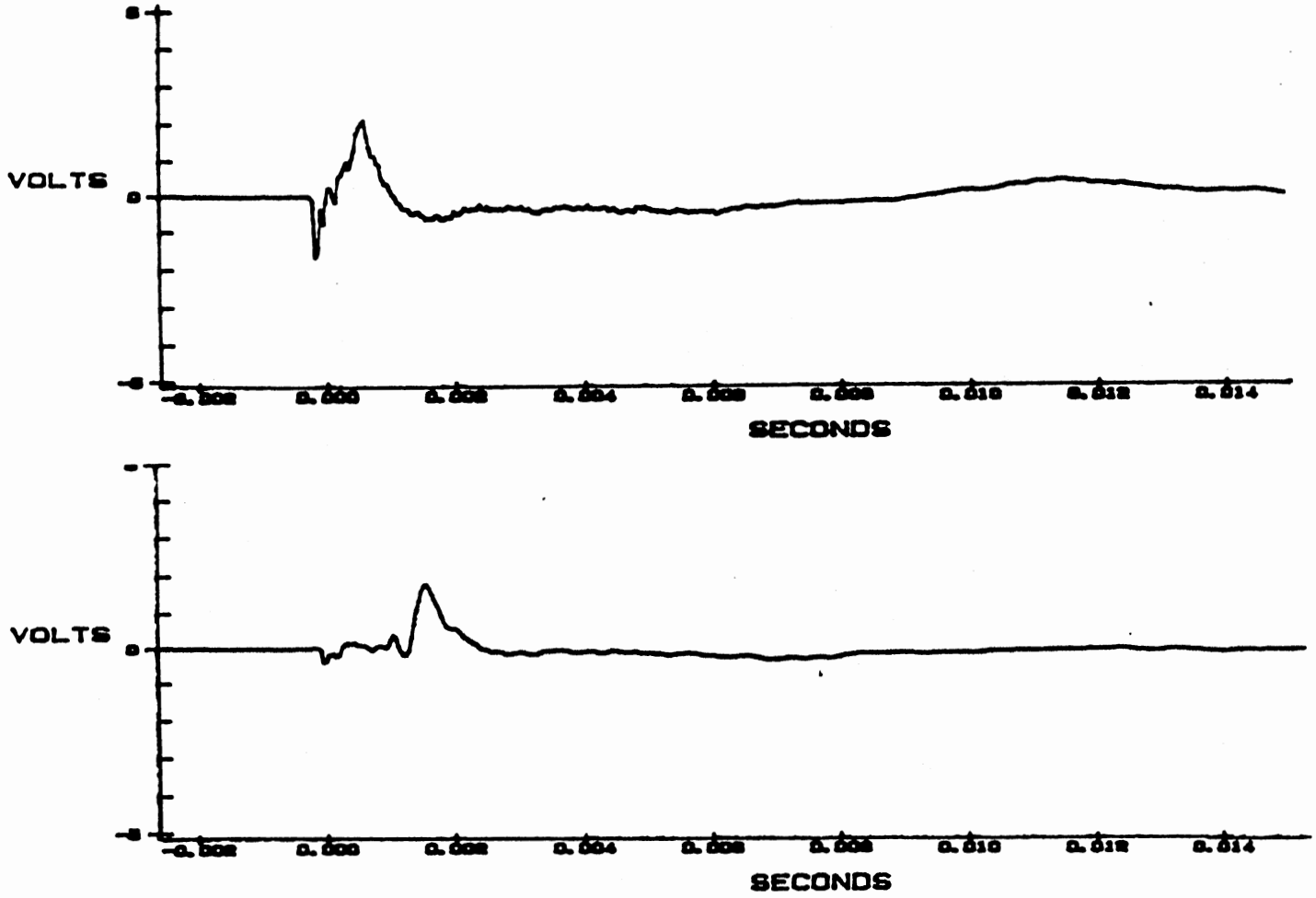

Figure 33. Signals From Differentiator/Inverter Circuit

back on. Therefore, an inverted square wave is generated; it is shown in Figure 34. The two signals are consistently at a voltage level of about -4 volts, so a counter-timer can trigger off of one wave and stop at the other wave, giving a time difference. However, some problems existed with the utilization of this waveform. The original wave fed into the Schmitt trigger must be rock-steady and must always be assured of giving 1.6 volts. The pneumatic pulser involved with this experiment had a tendency to "bounce" the web up and down. The signal was partially lost each time the web moved away from the microphones. Therefore, the waves tended to come and go, thus making timer measurements difficult.

Another problem with the Schmitt trigger waves was that the two input waves were different in height. The Schmitt trigger time difference measurement was from 1.6 volts to 1.6 volts, instead of peak to peak. The peak-to-peak time difference measurement is a more accurate means of determining tension. The time difference for Figure 34 was 1640 microseconds, which is much longer than the 1080-microsecond time difference for the original waves. If the original waves were the same shape and height and did not disperse, the Schmitt trigger would be more useful and effective.

For a moving web, one would expect the signals to have considerably more noise than the static web signals. However, the waves do not have much more noise than they do

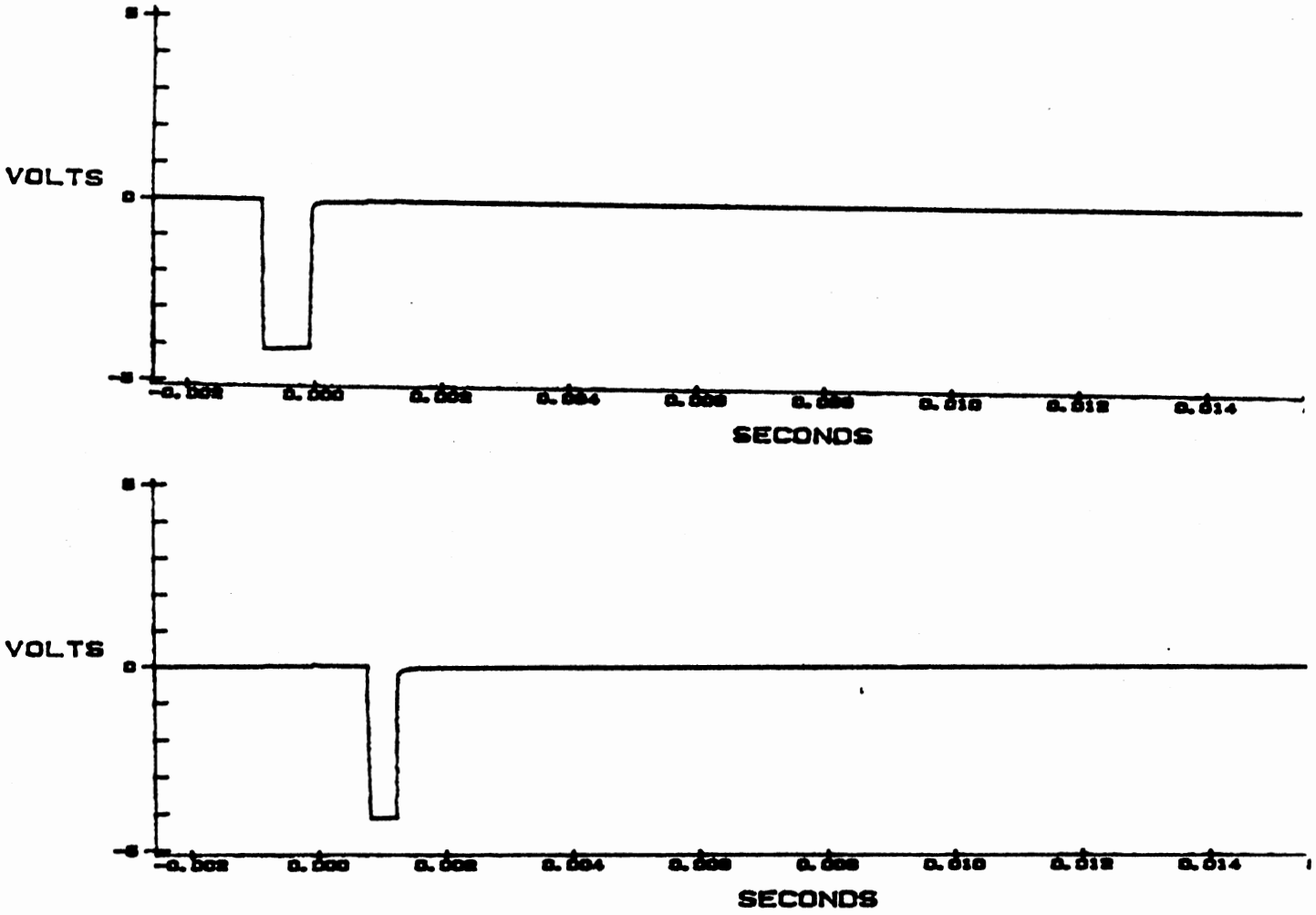

Figure 34. Signals From Schmitt Trigger Circuit

statically. An example is given in Figure 35, where the web was run at about 2070 feet per minute. The signal-to-noise ratio is quite high.

Signals from the Precision Diode Circuit are shown in Figure 36. The 6-inch metallized web was used, at a tension of 3.73 pli for this figure. The test was done statically using the original pneumatic pulser at an inlet pressure of 120 psi. The original pneumatic pulser produces very sharp, clean signals, as is seen from the figure. The Precision Diode Circuit eliminated most of the air spike and gave the signal a gain of 5.

Figure 37 shows the high-pass-filter output of the electric spark gap pulser. The 6-inch paper web was used at an average applied tension of 2.06 pli. After the pulse was transmitted onto the web, part of it reflected back down the tube, which caused the reflections in the signal. Also, the pulse was so sharp that it saturated the microphones, which can be seen in the first part of the signal. The saturation may have been caused by electromagnetic radiation noise. A long piece of plastic tubing was inserted into the tube over the capacitor to try to minimize reflections. However, this action caused the signal to die out before it reached the web. Another potential problem with the pulser is that it produces irregular pulses.

The spark gap pulser has good possibilities. It produces a sharp signal in the web. If reflections can be

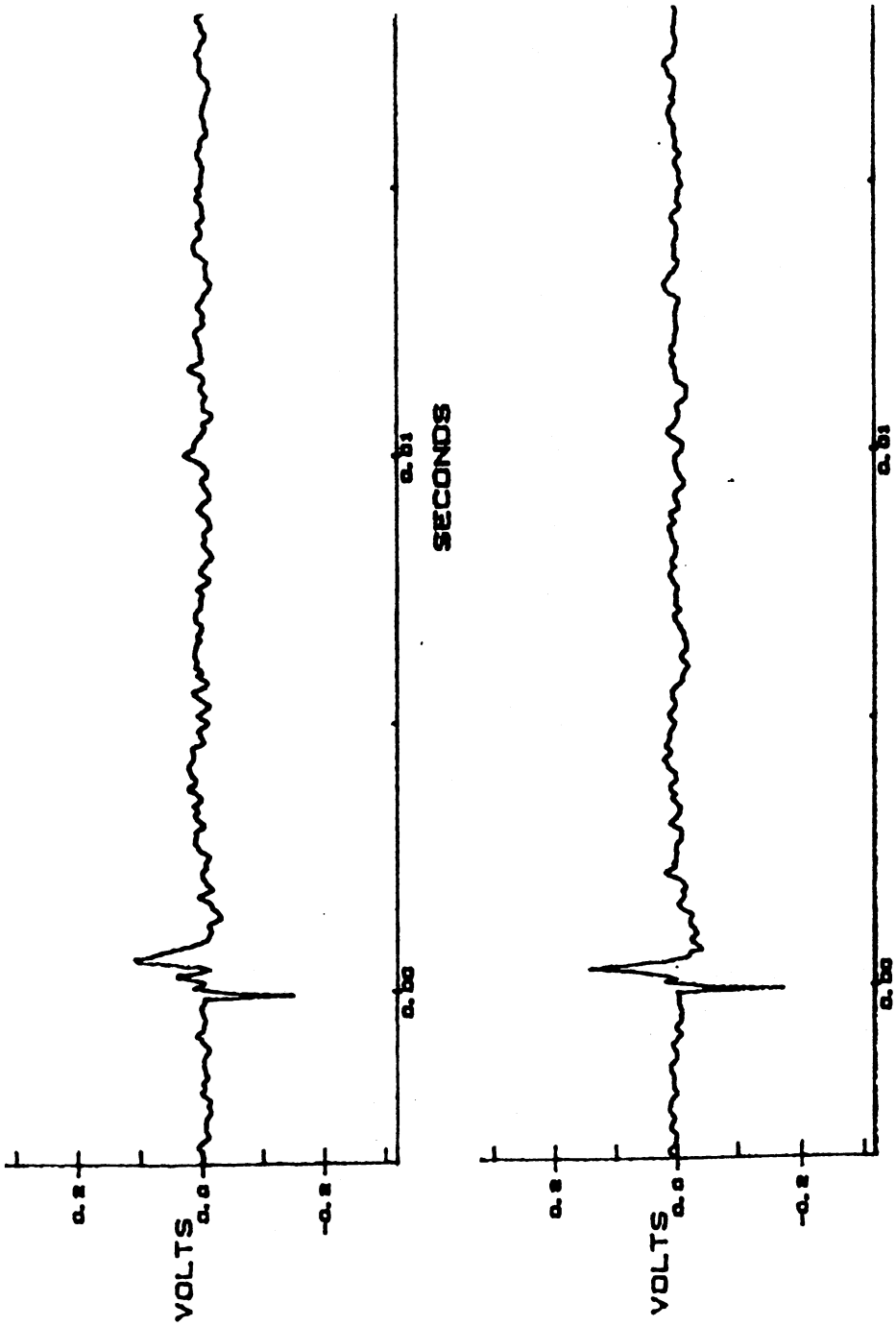

Figure 35. Signals for a Moving Web

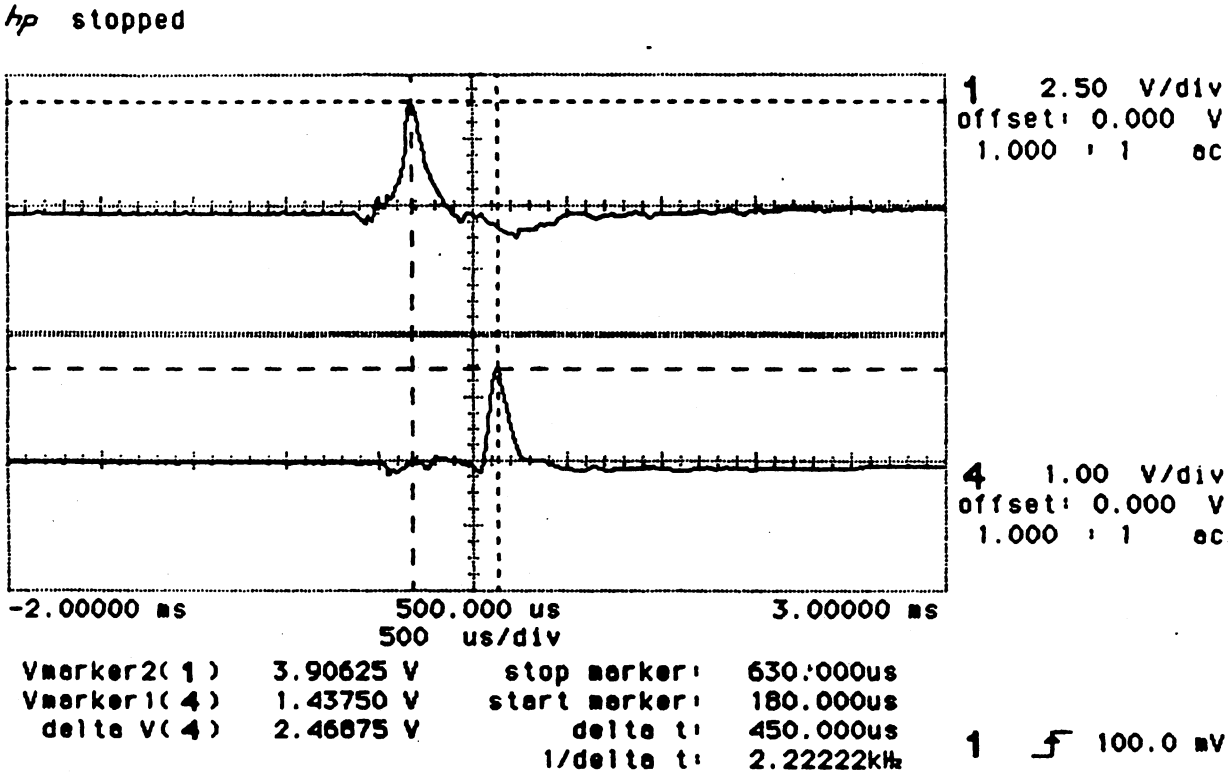

Figure 36. Signals From the Precision Diode Circuit

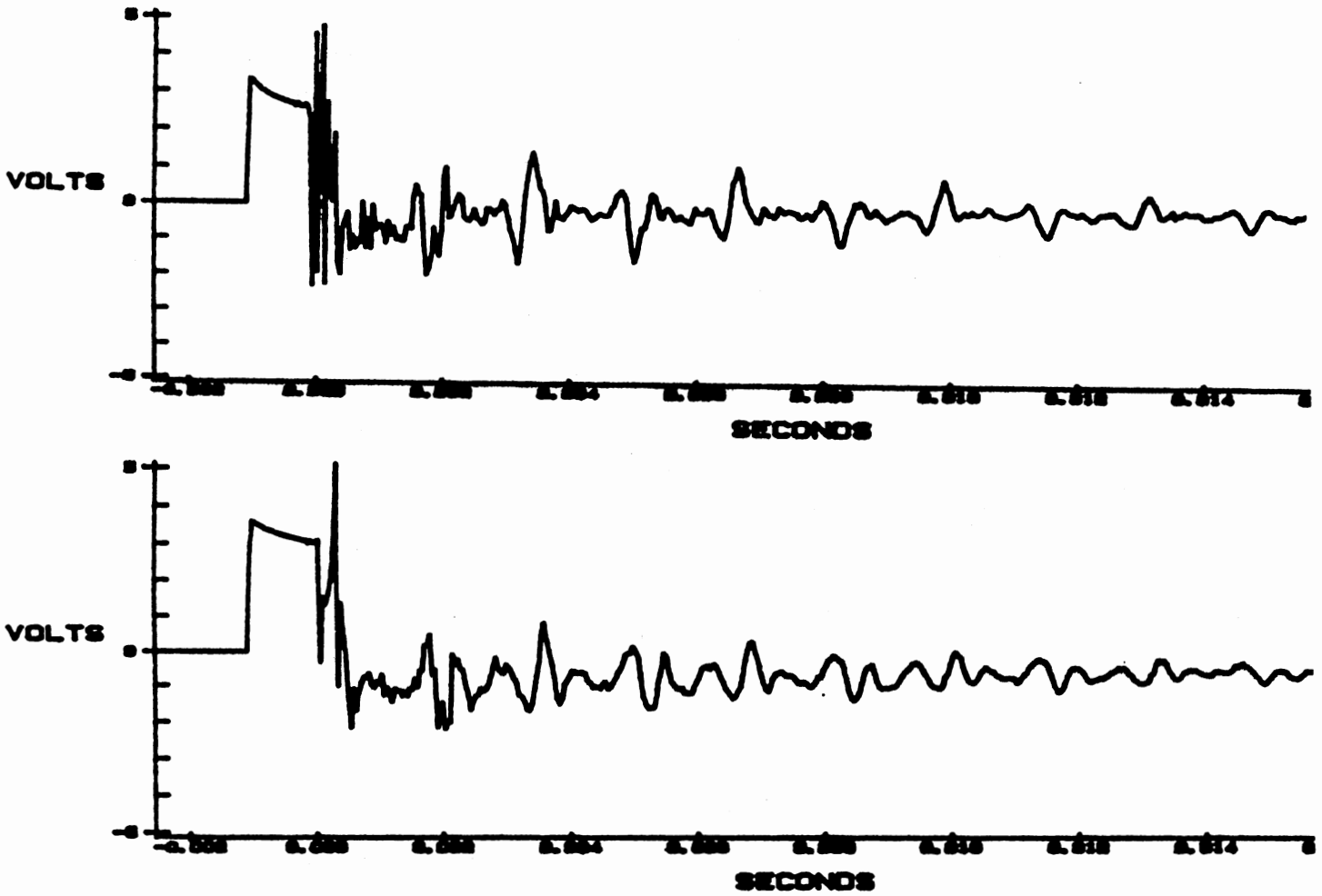

Figure 37. High-Pass-Filter Output From Spark Gap Pulser

minimized and a regular pulse produced. the electric spark gap pulser will be quite useful.

Determination of ρ_A

The term ρ_A was discussed in Chapter IV, Objectives. It was stated that

$$T = [(x/t) - V_w]^2 * (\rho_w + \rho_A)$$

where T is the tension. x is the distance between microphones, t is the time delay between signals, V_w is the web velocity, and ρ_w is the areal density of the web. The above equation can be solved for ρ_A as follows:

$$\rho_A = \frac{T_{avg}}{(x/t)^2} - \rho_w$$

The term ρ_A was determined by running a set of experiments, recording average tension and time differences. The spacing between microphones, x, was set at 2 inches. The test was done statically on the 6-inch metallized web, which had a basis weight (ρ_w) of 0.0068013 pounds mass per square foot. Two sets of experiments were done to obtain time delays, thereby giving a delta t from two sources: (1) an average of ten samples taken at one location on the web and (2) an average from one sample taken at six locations across the web.

The results of these experiments are tabulated in Table XIV in the Appendix. A graph of the results is shown in

Figure 38. Although the two values of ρ_A vary by as much as 29 percent at the lower tensions, they follow the same trend and get closer as tension increases. As is seen from the figure, ρ_A is not constant with tension. This variation is to be expected, because wavelength increases and frequency decreases with increasing tension. An attempt to use a ρ_A averaged over the tension range resulted in large errors of about 26 percent at low tensions. Therefore, the use of a lookup table for each material with different values of ρ_A for different tensions is recommended.

Comparison of Theoretical and Applied Tension

Tension was applied to webs via a weight distribution, so the tension applied was an average tension across the width of the web. In any place in the web, tension can actually be greater or less than the average tension: for example, a floppy edge would have less than average tension. Some experiments were run to compare calculated tension with average tension. The tension was calculated by the familiar equation for a static web:

$$T = (\rho_w + \rho_A) * (x/t)^2$$

where T is the tension, ρ_w is the basis weight of the web, ρ_A is the term which was determined in the previous section, and x/t is the wave speed in the web. An experiment was done in which one sample was taken at each tension in one

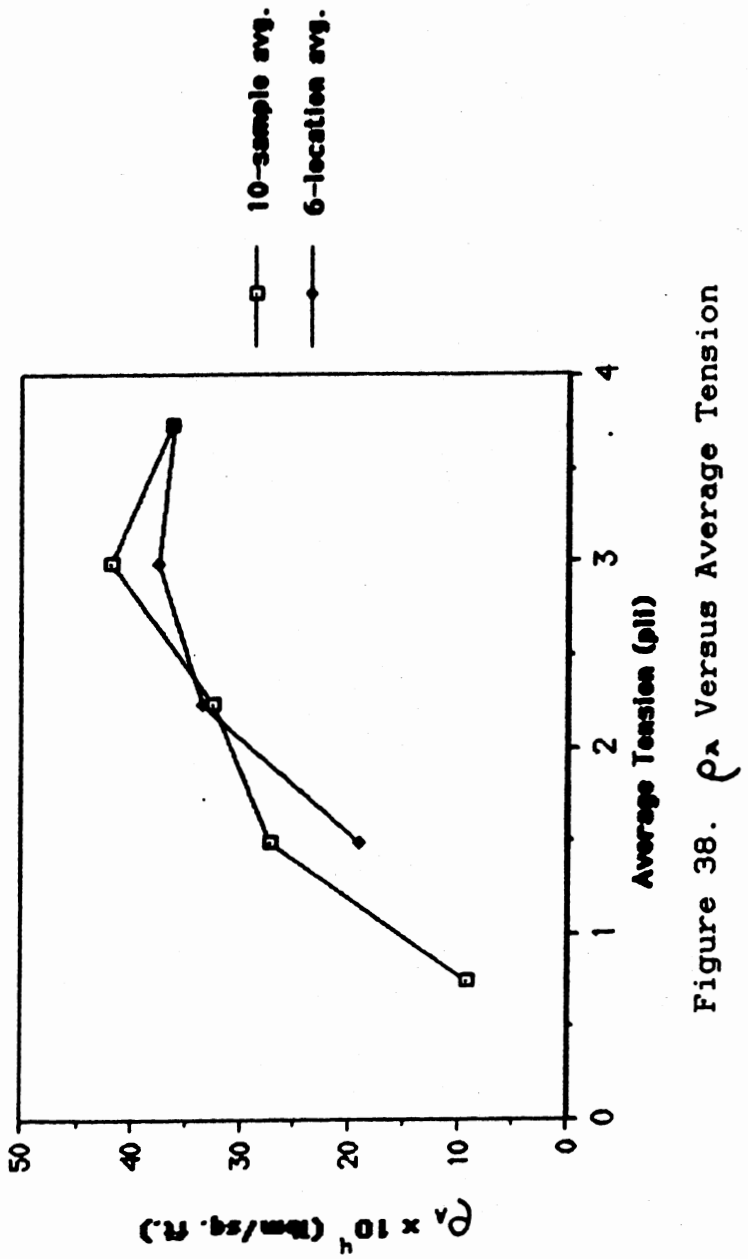

Figure 38. ρ_A Versus Average Tension

location of the aluminized web. The test was done statically using the original pneumatic pulser with a supply pressure of 130 psi. The Precision Diode Circuit was used on the signals.

Table XV of the Appendix shows how the tension measurements compare with the average tension. Figure 39 shows the corresponding data plot. It can be seen from the figure that the tension measurements are within 10 percent of the average tension, and they are consistently below the average tension. The measurements were probably made on a low-tension spot on the web, such as near a floppy edge. However, accuracy is probably improved if several time delay measurements are taken and averaged in one location on the web.

To see how average tension compares with averaged tension values, tension was calculated using the same formula and was then averaged. Two sets of data were taken at one tension at five locations across the 6-inch paper web. The original pneumatic pulser was used with an inlet pressure of 120 psi. The tension was maintained at 2.81 pli, and the distance between the pulser tube and web was about 0.1 inch.

The data are tabulated in Table XVI in the Appendix. Figure 40 illustrates the tension profiles for the two data sets. The data differ for the first and second data sets, possibly because the tension-measuring device was not in the

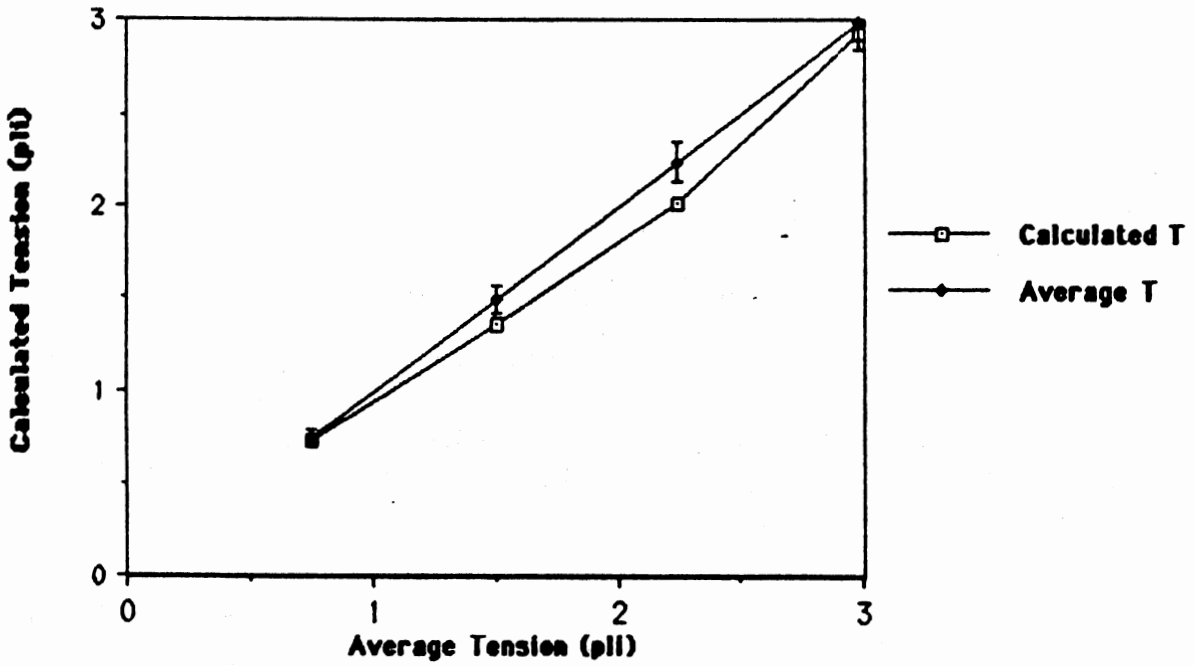

Figure 39. Comparison of Average Tension Versus Calculated Tension

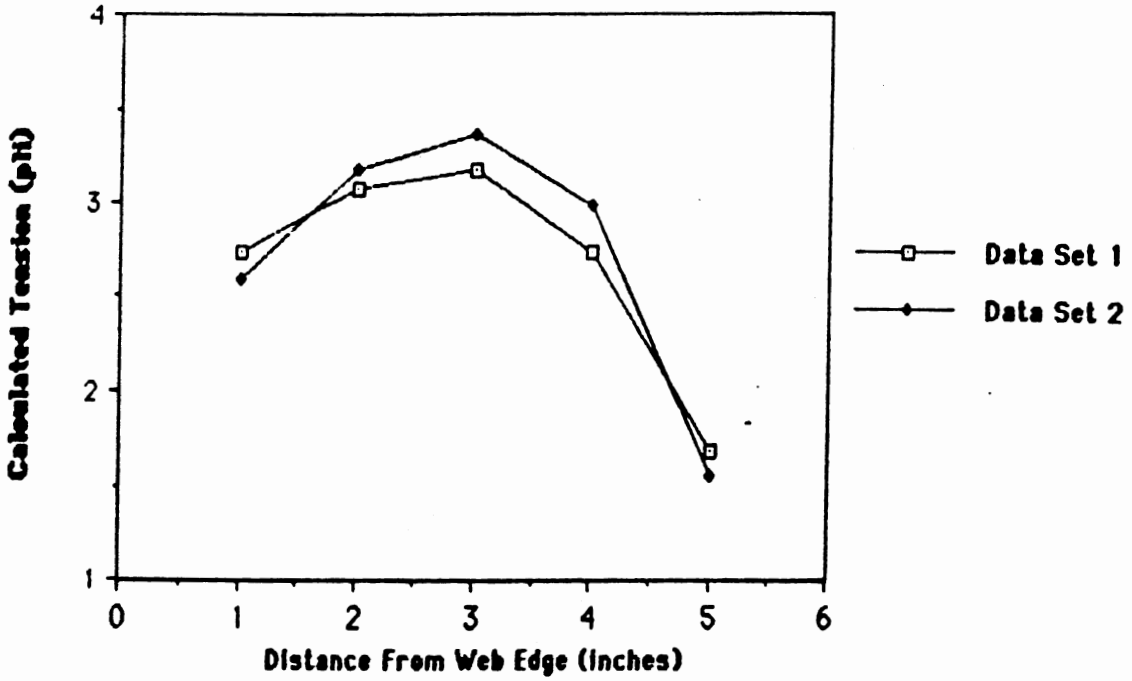

Figure 40. Tension Profiles for Two Sets of Data

exact same web location for the two experiments. However, the trends can still be compared.

For the first and second data sets, the highest tension occurred in the center of the web--higher than average tension by 13 and 20 percent, respectively. Also, the lowest tension for both data sets occurred on one edge of the web; it was 40 and 45 percent lower than the average tension for the first and second data sets, respectively.

When all five tensions were averaged together for each data set, the average tension for the first data set was 2.68 pli and for the second data set was 2.73 pli. These calculated average tensions are close to 2.81 pli, which was determined by the static model. The errors are 4.4 and 2.6 percent, respectively.

For this particular tension device, the tensions are much closer to average tension when the ρ_A term is included in the tension equation. This term accounts for the weight of air on the web and therefore must be considered.

CHAPTER VII

CONCLUSIONS AND RECOMMENDATIONS

The purpose of this study was to progress toward the development of a light, compact, hand-held tension-measuring device. The device is noncontact and can be used for static and moving webs. The signal-to-noise ratio is very high for the moving web. The device is also inexpensive.

The tension-measuring device is compact, being only 4 inches in length. This length was determined by the fact that the optimum microphone spacing was 2 inches. The signals disperse very little when they are picked up at such a short distance from the pulser tube. The recommended pulser mechanism is the original pneumatic pulser, which generates a clean, sharp pulse in the web and produces no reflections. The best circuit is the Precision Diode Circuit, which eliminates the negative air spike in the signal and gives it a gain of 5. The stiff, 1/4-inch plastic tubing works very well with the pneumatic pulser when its length is minimized. The electret microphone elements have a satisfactory frequency response for use with the pneumatic pulser.

The best time difference between signals is obtained when the signals are measured from peak to peak. The cross-

correlation is not recommended for these signals, because the slightly negative voltage at the beginning of the Precision Diode Circuit signals causes several oscillations in the cross-correlation. However, a rough cross-correlation could be used on the signals. The cursors on the Fourier analyzer and digital oscilloscope work fairly well for measuring time differences, but the instruments are limited in sampling rate. Therefore, the recommendation for measuring time differences is to digitize the signal using a computer with an analog-to-digital board with an extremely fast sampling rate. A program could be written to detect the peaks of the two signals, and delta t and tension could be printed out directly on the screen.

The use of the equation

$$T = (\rho_w + \rho_A) * [(x/t) - V_w]^2$$

is recommended for determining tension at any place in the web. This equation is used when the two microphones are placed downstream of the pulser and web velocity is in the same direction as the microphones. The term ρ_A is used as a calibration factor in this equation to account for air loading effects on the web. In this equation, T is tension, ρ_w is the basis weight of the web, ρ_A is the quantity determined in Chapter VI, x is the distance between microphones, t is the time difference between the two signals, and V_w is the web velocity. The term ρ_A was determined using the 6-inch metallized web and varied with

tension applied to the web. The recommendation is that ρ_A be listed in a lookup table for varying tensions. Using this equation, the point-source signal behaves like ribbon wave theory.

A load cell model was used to determine average tension applied to the web. The model involved some measurement of angles, which could have been a source of error. A propagating error analysis revealed that the error due to angle measurement could have been as high as 5 percent.

The wave velocities obtained experimentally were close to those obtained by the formulas for an air-loaded web. Therefore, the signal frequency was considerably lower than the 10 kilohertz necessary to use the equation for a web in vacuum. An average frequency estimated for the air-loaded web formulas was 1485 hertz. A sensitivity analysis for frequency revealed that using the constant, average frequency rather than a varying frequency for each tension produced very small deviations of less than 2 percent.

Wave height increased with increasing tension in all the experiments. This phenomenon may have occurred because the pulser tube was interacting with the web due to its close proximity. The wave height may therefore prove to be a reliable tension measurement criterion.

Recommendations for future work include digitizing the waves and using a peak detector to calculate the time difference. Tension may be a direct readout on the computer screen in this case. This idea may be the basis for a hand-

held device that directly reads out tension. Another possibility for peak detection is a circuit, which could also be used in a hand-held device.

Another possibility to be explored is the use of wave height as a tension-measuring method. The interaction between the pulser tube and the web must first be ascertained. A tiny pressure transducer could be inserted into the tube to measure pressure at the tube exit. The wave height phenomenon may prove to be similar to the principle used by the nozzle-flapper displacement transducer.

Web excitation using the electric spark-gap pulser needs to be pursued. This method of excitation may produce higher frequencies than the pneumatic pulsers and thus may make it possible to use the tension equation for a web in vacuum:

$$T = \rho_w * c_w^2$$

First, however, the reflections produced in the pulser tube must be minimized. A pulse produced at consistent time intervals would also be helpful. Different sensors need to be explored because the electret microphone elements were saturated by the signal.

Another recommendation is to try an array of microphones across the web rather than a traversing mechanism. Tensions could then be monitored at several places across the web at the same instant in time. A

pneumatic pulser with a slot in the revolving disk could be constructed to produce several air pulses at once.

BIBLIOGRAPHY

1. Walbaum, H. Heinz, and Lisnyansky, Khaim, "Sensor Development: Review of Process Control Instruments for Measuring Paper Quality Variables, Part 2." Paper Trade Journal, Vol. 167, No. 14, August 15, 1983, pp. 34-40.

2. Hansen, Age, "A Portable Instrument for Web-Tension Control and Cross-Profile Recording." Tappi Journal, Vol. 69, No. 12, December 1986, pp. 48-51.

3. Meinander, Sven, and Marttinen, Tapio, "Measuring of Web Tension using Contactless Tension Meter." Graphic Arts Finland, Vol. 11, No. 1, 1983, pp. 34-36.

4. Karlsson, Hakan, and Strom, Valter, "STFI's Web Tension Indicator." Swedish Forest Products Research Laboratory, Appendix 2, 1986.

5. Marttinen, Tapio, and Luukkala, Mauri, "An Acoustic, Noncontacting Instrument to Measure Tension in a Moving Paper Web." 1985 IEEE Ultrasonics Symposium, pp. 553-556.

6. Rye, Timothy W., "Using TENSCAN to Measure the Tension Profile." TAPPI Proceedings, 1988 Finishing and Converting Conference, pp. 175-178.

7. Linna, Hannu, and Moilanen, Pertti, "Comparison of Methods for Measuring Web Tension." Tappi Journal, October 1988, pp. 134-138.

8. Lee, Jaihak, "Wave Propagation Velocity of an Air-Loaded Web." Unpublished Oklahoma State University Master's Thesis, December 1986.

9. Francis, Glen D., "Normal Wave Propagation Velocity in a Static Web." Unpublished Oklahoma State University Master's Report, December 1986.

10. Nutter, Darin W., "Investigation of Experimental Noncontact Tension Measurement Methods." Unpublished Oklahoma State University Master's Report, May 1988.

11. Merilainen, Pekka, "Propagation and Excitation of Membrane Waves Loaded by Air." IEEE Journal on Microwaves, Optics and Acoustics, Vol. 2, No. 5, September 1978, pp. 147-152.

12. Soluyan, S. I., and Khokhlov, R. V., "Propagation of Acoustic Waves of Finite Amplitude in a Dissipative Medium." Nonlinear Acoustics in Fluids, Robert T. Beyer, ed., Van Nostrand Reinhold Company, 1984, p. 193.

13. Doebelin, Ernest O., Measurement Systems: Application and Design. Third Edition, McGraw-Hill Book Company, 1983, p. 289.

14. Beckwith, Thomas G.; Buck, N. Lewis; and Marangoni, Roy D., Mechanical Measurements. Third Edition, Addison-Wesley Publishing Company, 1982, pp. 269-270.

APPENDIX

TABLES FOR CHAPTER VI

TABLE I

WAVE HEIGHT AND WIDTH DATA ARRANGED WITH VARYING DISTANCE FROM WEB EDGE

Distance From Web Edge (inches)	Wave Heights (mV) 0.663 pli	1.33 pli	1.99 pli	2.65 pli	3.31 pli
1.0	165.626	176.563	195.313	193.750	200.000
2.0	168.750	178.125	196.875	203.125	212.500
3.0	131.250	159.375	168.750	181.250	193.750
4.0	134.375	146.875	146.875	175.000	178.125
5.0	109.375	134.375	134.375	153.125	171.875

Distance From Web Edge (inches)	Wave Widths (usec) 0.663 pli	1.33 pli	1.99 pli	2.65 pli	3.31 pli
1.0	370.000	330.000	340.000	270.000	220.000
2.0	330.000	310.000	280.000	270.000	230.000
3.0	310.000	270.000	250.000	250.000	230.000
4.0	380.000	330.000	260.000	270.000	280.000
5.0	380.000	310.000	320.000	280.000	250.000

TABLE II

WAVE HEIGHT AND WIDTH DATA ARRANGED
WITH VARYING AVERAGE TENSION

	Wave Heights (mV)				
Average Tension (pli)	x = 1 Inch	x = 2 Inches	x = 3 Inches	x = 4 Inches	x = 5 Inches
0.66	165.626	168.750	131.250	134.375	109.375
1.33	176.563	178.125	159.375	146.875	134.375
1.99	195.313	196.875	168.750	146.875	134.375
2.65	193.750	203.125	181.250	175.000	153.125
3.31	200.000	212.500	193.750	178.125	171.875

	Wave Widths (usec)				
Average Tension (pli)	x = 1 Inch	x = 2 Inches	x = 3 Inches	x = 4 Inches	x = 5 Inches
0.66	370.000	330.000	310.000	380.000	380.000
1.33	330.000	310.000	270.000	330.000	310.000
1.99	340.000	280.000	250.000	260.000	320.000
2.65	270.000	270.000	250.000	270.000	280.000
3.31	220.000	230.000	230.000	280.000	250.000

TABLE III

DATA FOR STATIC VERSUS MOVING WEB

Average Tension (pli)	Average Height (mV)		Delta V (mV)	
	400 fpm	Static	400 fpm	Static
1.65	86.458	72.917	25.000	18.750
2.48	93.750	77.083	12.500	9.375
3.30	97.917	68.750	34.375	15.625
4.13	92.708	84.375	18.750	15.625
4.95	102.083	91.667	34.375	12.500

TABLE IV

PULSE HEIGHT VERSUS PULSER
TUBE DISTANCE FROM WEB

Pulser Tube Distance From Web (inches)	Wave Height at Location 1 (mV)	Wave Height at Location 2 (mV)
0.023	128.125	109.375
0.045	137.500	115.625
0.086	137.500	112.500
0.123	131.250	109.375
0.140	115.625	112.500
0.172	121.875	115.625
0.201	128.125	115.625
0.228	118.750	128.125

TABLE V

WAVE HEIGHT VERSUS PRESSURE DATA

Pressure (psi)	Wave Height (mV)
60	103.126
70	135.938
80	168.751
90	234.376
100	290.626
110	342.188
120	412.501

TABLE VI

WAVE HEIGHT DATA FOR TWO MICROPHONES

Average Tension (pli)	Wave Height, Microphone 1 (mV)	Wave Height, Microphone 2 (mV)
1.40	290.625	309.375
2.10	300.000	365.625
2.81	290.625	384.375
3.51	412.500	478.125

TABLE VII

DATA FOR WAVE HEIGHT VERSUS
DISTANCE FROM WEB EDGE

Distance From Web Edge (inches)	Wave Height, Microphone 1 (mV)	Wave Height, Microphone 2 (mV)
1.0	300.000	346.875
2.0	450.000	534.375
3.0	365.625	450.000
4.0	346.875	290.625
5.0	262.500	215.625

TABLE VIII

HIGH-PASS-FILTER DATA AT 550 FPM

Average Tension (pli)	Minimum Wave Height (V)	Maximum Wave Height (V)	Average Wave Height (V)	Change in Wave Height (V)
1.40	2.00000	3.15625	2.52083	1.15625
2.10	1.81250	3.65625	2.64583	1.84375
2.81	2.18750	3.50000	2.88542	1.31250
3.51	2.53125	3.28125	2.94792	0.75000
4.21	2.78125	3.96875	3.37500	1.18750

TABLE IX

COMPARISON OF WAVE SPEEDS CALCULATED FROM AVERAGE DELTA T, ROOT T/ρ, AND AIR-LOADED WEB FORMULAS

Average Tension (pli)	Wave Speed From Average Delta T (in/sec)	Wave Speed, Root T/ρ (in/sec)	Wave Speed From Air-Loaded Web Formulas	
			Microphone 1 (in/sec)	Microphone 2 (in/sec)
0.75	2317	2470	2088	2065
1.49	2950	3493	2739	2912
2.24	3515	4278	3332	3547
2.98	3883	4939	3710	4008
3.73	4454	5522	4080	4400

TABLE X

COMPARISON OF WAVE SPEEDS USING VARYING AND CONSTANT WAVELENGTHS

Average Tension (pli)	Wave Speed From Average Delta T (in/sec)	Air-Loaded Web Wave Speed With Varying Wavelength (in/sec)	Air-Loaded Web Wave Speed With Constant Wavelength (in/sec)	Percent Deviation, Constant Versus Varying Wavelength
0.75	2317	2088	2075	0.623
1.49	2950	2739	2791	1.900
2.24	3515	3332	3304	0.840
2.98	3883	3710	3716	0.162
3.73	4454	4080	4065	0.368

TABLE XI

TENSION PROFILE EXPERIMENTAL
WAVE SPEEDS

Distance From Web Edge (inches)	Tension (pli)	Delta t From Cursor (usec)	Wave Speed From Delta t (in/sec)
0.5	1.49	640	3125
	2.24	580	3448
	2.98	510	3922
	3.73	450	4444
1.5	1.49	710	2817
	2.24	600	3333
	2.98	520	3846
	3.73	450	4444
2.5	1.49	660	3030
	2.24	570	3509
	2.98	510	3922
	3.73	440	4545
3.5	1.49	640	3125
	2.24	550	3636
	2.98	500	4000
	3.73	450	4444
4.5	1.49	630	3175
	2.24	580	3448
	2.98	500	4000
	3.73	450	4444
5.5	1.49	610	3279
	2.24	550	3636
	2.98	490	4082
	3.73	450	4444

TABLE XII

COMPARISON OF AVERAGED TENSION PROFILE WITH KNOWN AVERAGE TENSION

Average Tension (pli)	Averaged Values of Tension Profile (pli)	Percent Deviation
1.49	1.84	22.9
2.24	2.52	12.4
2.98	3.39	13.7
3.73	4.49	20.4

TABLE XIII

VARIATION IN TENSION BETWEEN TWO WAVES FOR TWO SETS OF DATA

Distance From Web Edge (inches)	Tension (pli)		Percent Deviation
	Test 1	Test 2	
1.0	2.70	2.56	5.3
2.0	3.03	3.12	3.0
3.0	3.12	3.32	6.2
4.0	2.70	2.94	8.9
5.0	1.66	1.52	8.2

TABLE XIV

ρ_A AS DETERMINED BY TWO DIFFERENT METHODS

Average Tension (pli)	ρ_A From One Location, Ten-Sample Average (lbm/ft^2)	ρ_A From One-Sample, Six-Location Average (lbm/ft^2)
0.75	0.0009225	No data
1.49	0.0027332	0.0019171
2.24	0.0032716	0.0033662
2.98	0.0042010	0.0037779
3.73	0.0036524	0.0036214

TABLE XV

COMPARISON OF TENSION MEASUREMENTS WITH AVERAGE TENSION USING SEVERAL TENSIONS, ONE LOCATION

Average Tension (pli)	Delta t (usec)	Calculated Tension (pli)	Percent Deviation
0.75	880	0.78	3.8
1.49	710	1.36	8.8
2.24	600	2.01	10.1
2.98	520	2.93	1.9

TABLE XVI

COMPARISON OF TENSION MEASUREMENTS WITH AVERAGE TENSION OF 2.81 PLI USING ONE SAMPLE AT FIVE LOCATIONS ACROSS THE WEB

Delta t (usec)	Calculated Tension (pli)	Percent Deviation From Average Tension	Average of Five Tension Values (pli)
Experiment 1:			
720	2.74	2.2	
680	3.08	9.6	
670	3.17	12.9	2.68
720	2.74	2.2	
920	1.68	40.0	
Experiment 2:			
740	2.60	7.4	
670	3.16	12.9	
650	3.37	20.0	2.73
690	2.99	6.5	
960	1.54	45.0	

VITA

Marla Enfield Bradley

Candidate for the Degree of

Master of Science

Thesis: NONCONTACT TENSION MEASUREMENT IN WEBS BY ACOUSTICAL POINT-SOURCE EXCITATION

Major Field: Mechanical Engineering

Biographical:

Personal Data: Born in Billings, Oklahoma, February 17, 1959, the daughter of Harold O. and Ethel A. Enfield; married to Robert F. Bradley May 14, 1988.

Education: Graduated from Billings High School, Billings, Oklahoma, in May 1977; received two-year certificate in Stenography from Oklahoma State University in May 1979; received Bachelor of Science Degree in Mechanical Engineering from Oklahoma State University in May 1988; completed requirements for the Master of Science Degree at Oklahoma State University in December 1989.

Professional Experience: Word Processing Specialist, Information Processing Center, Conoco Inc., Ponca City, Oklahoma, October 1979 to August 1985; Research Assistant, Department of Mechanical Engineering, Oklahoma State University, June 1988 to December 1989.